Consolidation of Ground by Vertical Rope Drains

by

Dinesh Mohan*

G.S. Jain**

D.P. Sen Gupta***

Devendra Sharma*

Introduction

For improving the bearing capacity of soft strata preloading of ground has been used since long. But in the case of clayey soil strata of low permeability the gain in shearing strength is at a very slow rate and the loads should remain in position for long periods. For quicker consolidation, sand drains, known as sand piles also has been in use for quite some time. They accelerate the process of consolidation by providing easy drainage path. The first reported example of sand drains is on an-Fransico Oakland Bay Bridge (Porter, 1936). The installation of sand-drains is normally done by closed end driven pipes which are withdrawn after filling in the sand. The drawbacks of the process are the large scale handling of sand which is very often required to be brought from long distances, reduction in drainage efficiency known as 'smear effect' and shear failures in the event of rapid preloading.

To replace the sand drains there has been the development of cardboard drains on which the first large scale experiment was conducted in Sweden in 1937 (Kjellman, 1948). The section of these drains was 100 mm $\times$ 3 mm and the installation was at much closer spacing (De Beer et al, 1974) than the sand drains. Various natural and synthetic materials are in use for making the drains of this type. The shortcomings of the process in Indian context are highly sophisticated and patented techniques of manufacture and installation and initial heavy investments.

In India another version of sand drains, known as 'sand wicks' was developed (Dastidar et al, 1969). The sand wicks formed by filling sand in long cylindrical hessian bags of about 65 mm diameter were installed with the help of 100 mm diameter casing pipe. Similar to cardboard wicks the principle utilised in sandwicks was that the effect of drain diameter on degree of consolidation was only a nominal one as compared to the spacing of drains (Leonard, 1962, Younger, 1968 and Rao et al, 1971). The driving was simpler but other shortcomings of sand drains still there. Further, the sandwicks had been reported more susceptible of a loss in their efficiency (Subbaraju et al, 1973).

---

*Director,

**Scientist co-ordinator,

***Scientist, Central Building Research Institute, Roorkee, India.

The paper is open for discussion till the end of October 1977.

Rope Drains

To overcome various shortcomings of the known processes and keeping in view the fact that closer spacing of drains is advantageous 'rope drains' were developed at the Central Building Research Institute, Roorkee, (Dinesh Mohan et al 1972). The material used was coir fibre which is a byproduct abundantly available in India. The coir is durable and strong in underwater conditions. The coir fibre is woven in the form of a long strip of mat about 150 mm wide and 10 mm thick and then rolled to give a hollow cylinderical tube, Figure 1, which is flexible like a rope. The outer effective diameter of

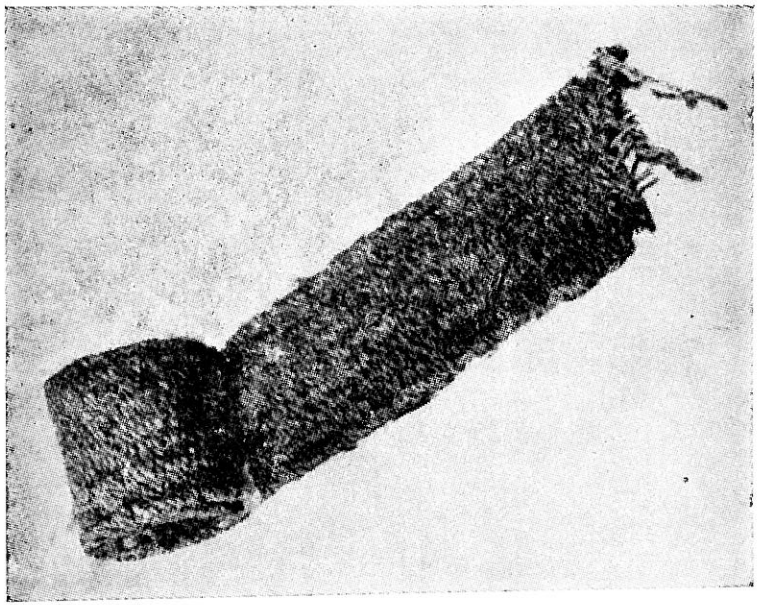

FIGURE 1(a): Coir mat strip

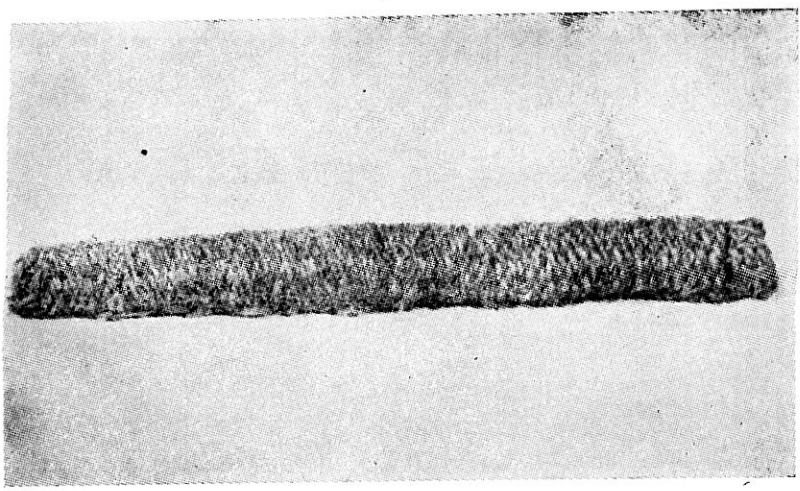

FIGURE 1(b): A piece of drain

the rope drain is about 70 mm and unlike sand drains and wicks, there is a continuous hollow space at its centre longitudinally.

Water draining efficiency of these drains is very good. Laboratory tests on coir fibre packed to a dry density of 0.5 gm per cu. cm showed permeability value of about 3×10^{-2} cm/sec. The coefficient of permeability of this order is comparable to that of clean sands (Terzaghi and Peck, 1967) and can be considered an effective substitute for sand used in sand piles. The permeability of treated card-bored drain is of the order of 10^{-5} cm/sec only (Kjellman, 1948).

For ascertaining the behaviour of rope drains in contact with consolidating soft soil laboratory tests were carried out in a triaxial cell. The soft clay was in direct contact with the circular coir drain and was contained in a rubber membrane. (Figure 2). The soil used in the experiment was

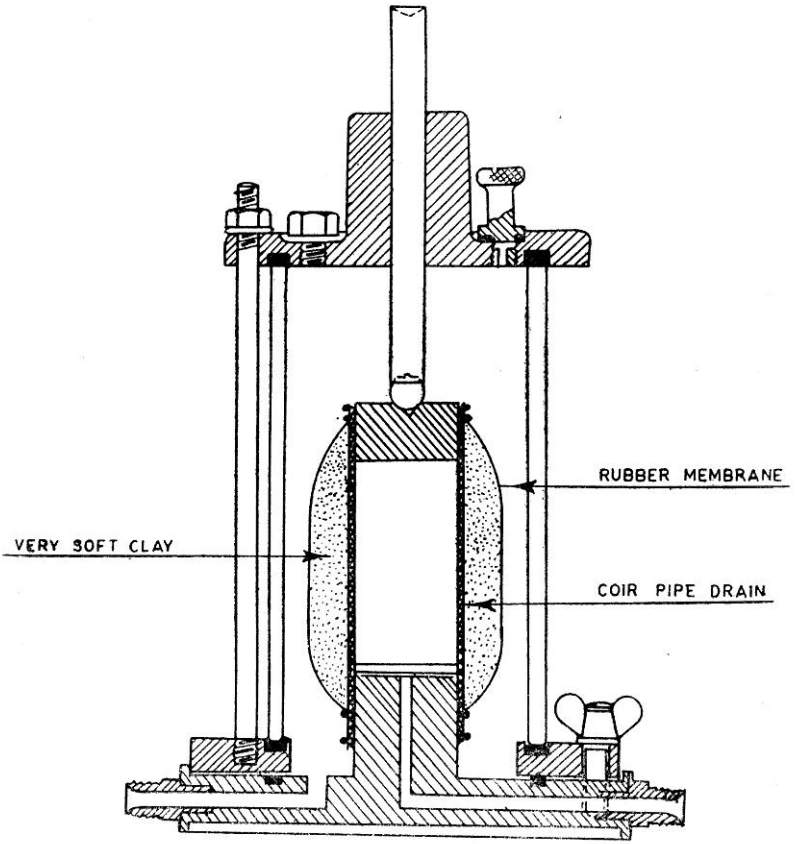

FIGURE 2. Triaxial cell test set up for coir pipe drain

of liquid limit 49 and plasticity index 27. The water content was close to liquid limit. A cell pressure of about 1.5 kg/cm² was applied which compressed the soft soil and led to its water being squeezed through the coir drain. It was observed that the clay did not penetrate beyond a thin skin on the out side of the coir drain and only clear water emerged on the other side. It was therefore concluded that under normal soft ground conditions, coir drains will prove satisfactory for rapid consolidation.

Field Trial

A full scale field trial was carried out at salt lake in Calcutta. A total number of 56 rope drains were installed in a square grid pattern of 8×7 in an area of 11.0 m $\times$ 12.8 m. The spacing of drains was about 1.83 m (Figure 3).

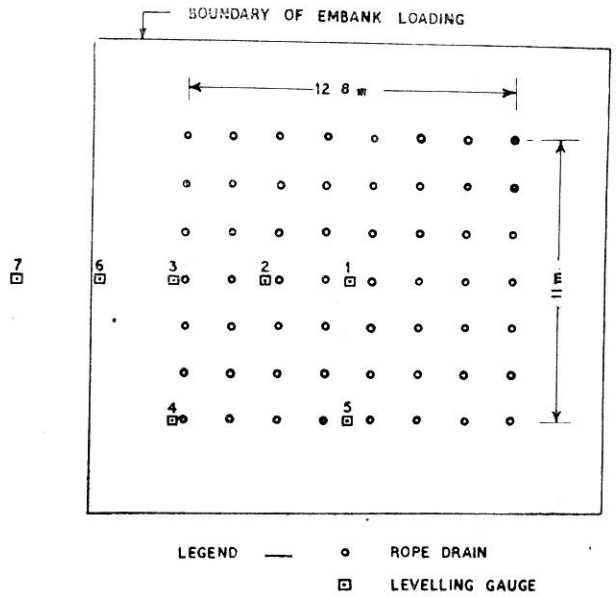

FIGURE 3. Layout of drains and gauges

The rope drains were installed by driving a 8 cm diameter pipe having a loosely fitting conical cast iron shoe at its bottom. Before driving the casing one end of the rope drain was securely tied to the hook in the conical shoe and the rope made to pass through the casing pipe of predetermined length. The driving head was suitably modified by providing a window on side so that rope drain is not damaged during driving. A 500 kg hammer operated by a rope and winch arrangement was used.

When the driving to the desired depth was over, the casing pipe was withdrawn, leaving conical shoe and the rope drain attached to it in position. The driving operation was simple and an ordinary tripod with a suitable winch arrangement was found adequate to install 70 mm diameter rope drains to 12.2 m depth. During an eight hours working five drains could be installed.

The soil strata consisted of a top layer of about 2 m poorly graded fine to medium sand followed by about 3.5 m of silty clay (*CL*) which was underlain by silty clay layers of higher plasticity (*CH*). At about 11.5 m depth the strata was stiff silty clay having some kankar. The bore logs and the penetration test data are shown in Figure 4 and other properties are summarised in Figure 5. It may be noted that silty clay stratum between 5 m and 11 m is generally soft with moisture content between liquid and plastic limit values. As the penetration resistance starts

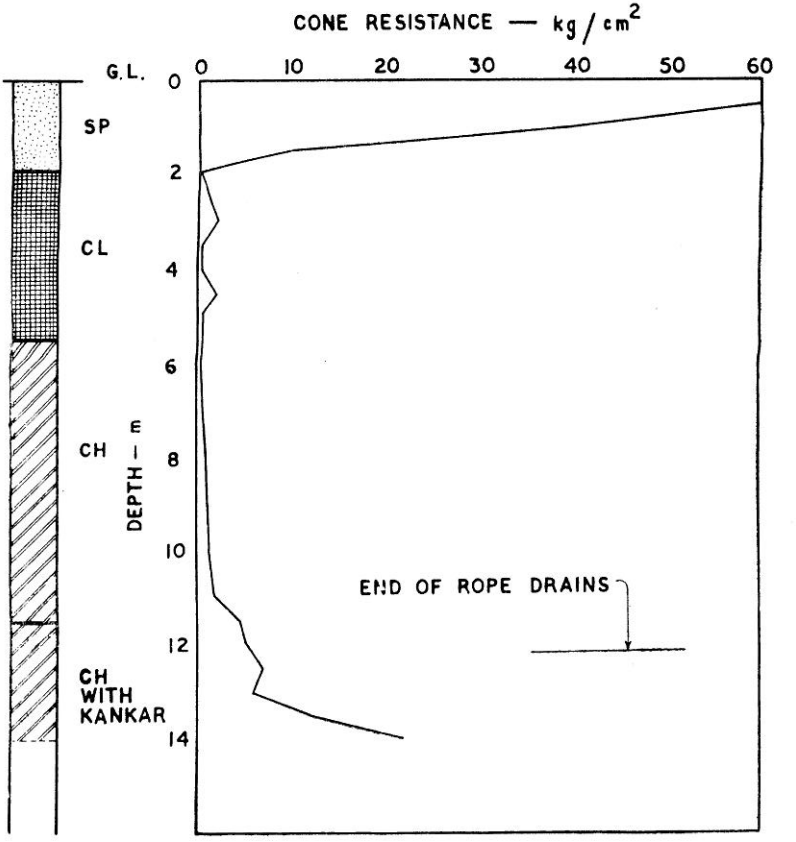

FIGURE 4. Bore log and static penetration resistance

improving steadily after 11 m, a depth of 11.2 m was decided for installing the rope drains.

After installation of drains the area was loaded (Figure 6) by sand embankment and a height of 3.75 m was achieved in 20 days (Figure 7). The final embankment loading gave a pressure intensity of 0.5 kg/cm². The base of the embankment extended beyond the boundary line of rope drains by about 2 m.

For recording the progress of settlement five level points were established at ground level within the rope drain area and two were outside (Figure 3). The level points consisted of an iron base plate of 30 cm × 30 cm to which a 20mm diameter conduit was attached and was sleeved by a 50 mm diameter pipe to avoid direct contact with the soil. Figure 3 shows a view of the embankment along with the levelling points. Similar arrangement has been used by other workers (Mehra and Natarajan, 1962). The reference datum was a 6 m high G.I. pipe fixed to an underreamed pile of 14 m depth at about 10 m away from the embankment. The levels were taken by a water tube level. As the levelling points were high above the embankment, an improvised bamboo staging was erected to support the

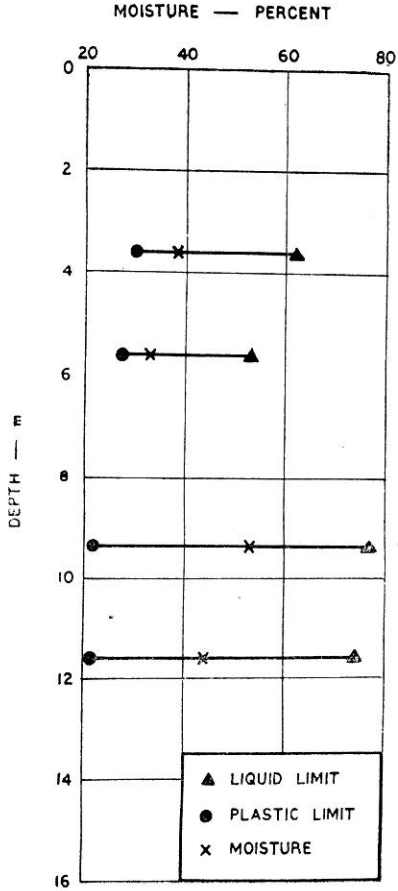

FIGURE 5. Soil properties

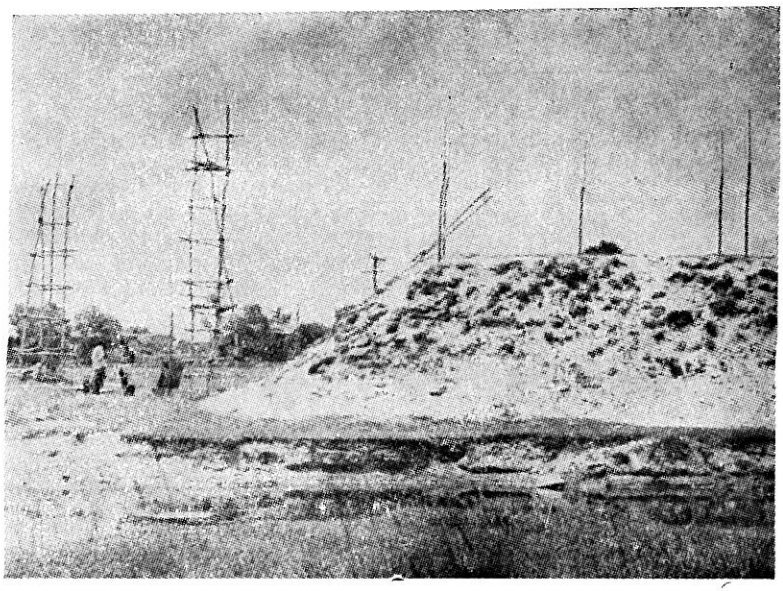

FIGURE 6. A view of embankment

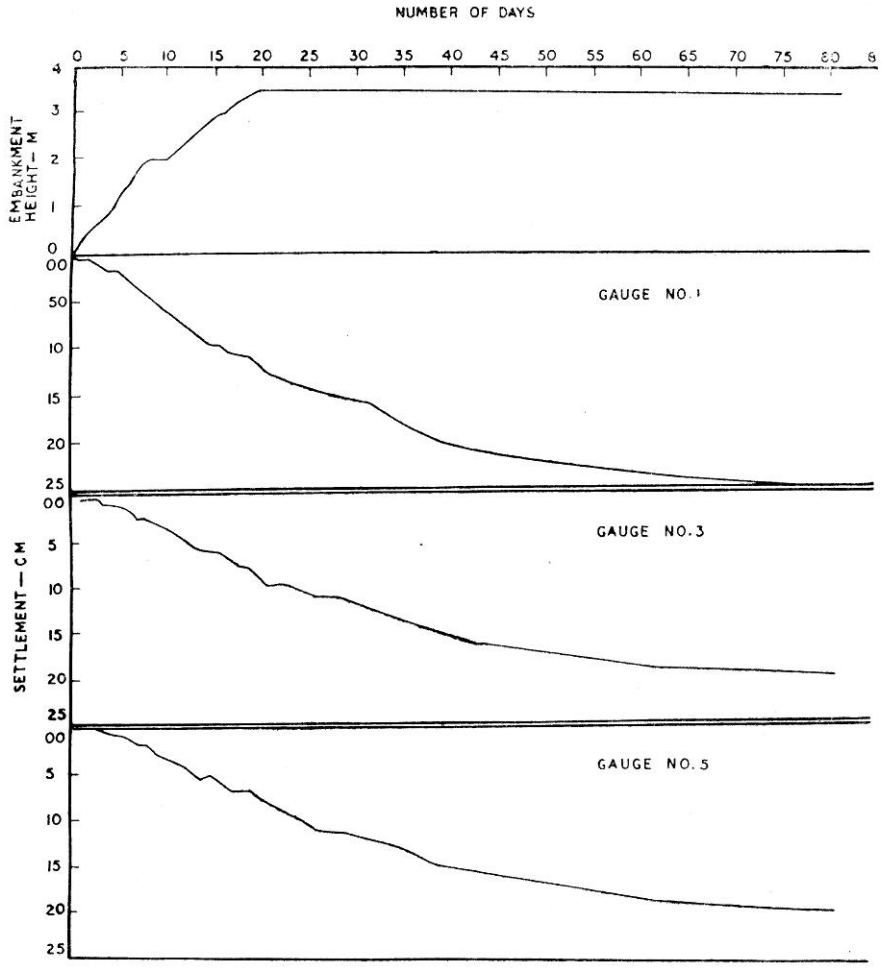

FIGURE 7. Progress of loading and settlement

water reservoir of the water tube level. The progress of settlement recorded at levelling point nos. 1, 3 and 5 is shown in Figure 7.

Discussion

For the layout of vertical drains two types of grid patterns, hexagonal and square are in practice. The hexagonal grid is said to be the most economical one (Barron, 1948). However, it is not a very important advantage (Kjellman, 1948). From practice it seems that while the sand drains are installed in a hexagonal grid, the small size drains like card board drains and sand wicks have been provided in a square grid. In our experiment on rope drains a square grid at 1.83 m spacing was adopted. The effective radius of influence zone was 1.03 m as the effective radius was 0.564 times the grid spacing (Younger, 1968).

The installation of drains by driving a pipe and its subsequent withdrawl can cause remoulding of the soil thereby reducing its permeability which

also is known as 'smear effect' (Barron, 1948; Richart 1957). Its effect is indirectly accounted for by considering a reduction in the well diameter and as an approximation it is said to be equivalent to halving the well radius (Leonard, 1962). Other workers (Rao and Rao, 1973) too have focussed attention on this aspect. In this context, as far as the rope drains are concerned, it may be noted that these are comparatively smaller diameter drains, (70 mm), and installation is done by a 100 mm diameter pipe. Hence, remoulding will be much less. Also the permeability of coir mat is very high and as shown by laboratory tests it functions as a draining material efficiently. The effect of smear may be pronounced in the case of distinctly horizontally layered soils. In clayey soils there is likely to be little effect on permeability (Kjellman, 1948). In view of these, it is felt that there is no need to consider smear effect in the case of rope drains.

For vertical drains theoretical solutions have been advanced for equal vertical strain and free strain conditions. In the latter case the soil surrounding the drains consolidates faster than the soil away from it. As has been stated earlier, rope drains are made of a coir mat having a hollow space all through their length. These are also flexible and are not likely to attract a greater intensity of load compared to the surrounding soil. The expected settlements will therefore be uniform and the case of equal vertical strains can be reasonably assumed to apply. It may be further noted that for ratios of effective diameter to drain diameter greater than 5, very close agreement is obtained between the equal strain and free strain cases (Younger, 1968). In the present case this ratio in about 30 and, consequently, the significance of these two conditions is not important.

The consolidating strata which will be significantly effected by rope drains lies between 2.0 to 12.2 m as the strata are comparatively much softer within these depths and top 2.0 m is sand. On the basis of compression index values which ranged from 0.24 to 0.79 the estimated total settlement of the 10.2 m clayey strata under an intensity of embankment loading of 0.5 kg/cm^2 at the centre is 28 cm. The observed settlement (Figure 7) after 81 days from the start of loading is 25 cm. The time-settlement curve has reached an almost asymptotic stage at this settlement which is about 90 per cent of the expected total settlement.

For calculation of settlement with the use of rope drains the charts developed by Barron (1948) relating time factor and degree of consolidation for various ratios of effective radius to drain diameter have been used.

The radius of well diameter (r_w) is 3.5 cm, the effective radius of influence zone (R) is 1.03 m. Hence the ratio $R/r_w=n$ is 29.5 (say 30). From laboratory consolidation tests the average value of coefficient of consolidation in vertical direction (c_v) was estimated to be 4.046×10^{-4} cm^2/sec. The ratio of horizontal to vertical permeability was taken about 2.3.

The degree of consolidation of three dimensional flow U, vertical flow U_v and radial flow U_r were considered (Carillo, 1942) related as

$$1-U=(1-U_v)\,(1-U_r)$$

In the present case the degree of consolidation of three dimensional flow, U, is 90 percent. By assuming various values of U_v, by trial and error, it can be shown that in the present case of $R_w=30$, $C_{vr}/C_v=2.3$, $R=1.03$ m, depth of strata $(H)=10.2$ m and $U=90$ percent the contribution by vertical consolidation is reflected by U_v of 13 percent only. If on the other hand 13 percent of the total consolidation were required to be achieved under the present intensity of loading without the use of drains, the time required will be about 400 days against the actual time 71 days. It is considered that full loading becomes effective after 10 days as there is almost linear increase upto 20 days (Figure 7). To realise 25 cm settlement without rope drains which is 90 percent of final expected, therefore a period of many years will be required. Thus the efficacy of rope drains for quicker settlements is obvious.

The gauge no. 6 near the foot of embankment and no. 7 at about 3 m away from it (Figure 3) did not show any heaving of the ground, which indicates that there was no lateral flow of the soil.

An analysis of cost showed that the major part of the cost was towards the loading and unloading of the soil for the embankment. In this trial the ratio of the cost of installation, the cost of material and the embankment was 1:2:9. In cases where the embankment loading was not required to be removed, such as for highway embankments, the cost of the last item will be almost halved.

Concluding Remarks

Laboratory experiments and field trial have shown that the rope drains made by rolling a coir strip have positive advantages over conventional sand drains and other types of vertical drain. The material used is highly permeable and the central hollow space ensures uninterrupted passage for drainage. The smaller diameter and lighter weight permits easier handling and driving. The flexibilty and strength safeguards against loss of continuity in an event of shear failure by excessive embankment loading. Closer spacing is possible to easy driving and it leads to increasing the efficiency of the process. The fabrication of rope drains as also their installation are simple and quick.

Acknowledgement

The study was carried out as a part of the normal research programme of the Central Building Research Institute.

References

BARRON, R.A., (1948), 'Consolidation of fine grained soils by drain wells' *Transactions of the ASCE*, Vol. 113, pp. 718-742.

CARILLO, N., (1942), 'Simple two and three dimensional cases in the theory of consolidation of soils', *Journal of Mathematics and Physics*, Vol. 21, p. 1.

DASTIDAR, A.G., GUPTA, S. and GHOSH, T.K., (1969), 'Application of sand wicks in a housing project' *Proceedings of the Seventh International Conference on Soil Mech. and Found. Engg.*, Mexico, Vol. 2, pp. 59-64.

DE BEER, E.E. et al, (1974), 'Accelerated Consolidation by means of cardboard Drains'. *La Technique des Travaux*, No. 346, March-April, pp. 3-8.

DINESH MOHAN et al., (1972), 'A Method of strengthening of soil', *Indian Patent No. 134557.*

KJELLMAN, W., (1948), 'Accelerating consolidation of fine grained soils by means of cardboard wicks', *Proceedings of the Second International Conference on Soil Mech. and Found. Engg.* Rotterdem, Vol. II, pp. 302-305.

KJELLMAN, W., (1948), Discussion on 'Consolidation of fine grained soils by drains wells' *Transactions of the ASCE*, Vol. 113, pp. 748-751.

LEONARDS, G.A., (1962), 'Foundation Engineering' *McGraw Hill Book Company*, Inc. New York, pp. 172-176.

MEHRA S.R. and NATRAJAN, T.K., (1962), 'Practical lessons in vertical sand drains installation' *Road Research papers*, No. 54, New Delhi, pp. 1-33.

PORTER, O.J., (1936), 'Studies of fill construction on mud flats including a description of experimental construction using vertical sand drains', *Proceedings of the first International Conference on Soil Mech. and Found. Engg.*, Cambridge, Vol. 1, pp. 229-235.

RICHART, F.E., (1959), 'Review of the theories of sand drains' *Transactions of the ASCE* Vol. 124, pp.709-736.

RAO, D.B. and RAO, D.B., (1973), 'Effects of smear in sand drains' *Indian Geotechnical Journal*, Vol. 3, No. 4, pp. 285-293.

RAO, D.J., MADHAV, M.R. and RAO, K.K., (1971), 'Design procedures for sand drains', *Journal of the Institution of Engrs.* (India) Vol. 51, No. 9, Pt CI 5, pp. 235-239.

SUBBARAJU, BH., NATRAJAN, T.K. and BHANDARI, R.K., (1973), 'Field performance of drain wells designed expressly for strength gain in soft marine clays' *Proceedings of the eighth International Conference on soil Mech. and Found. Engg. Moscow*, Vol. 2, pp. 217-220.

Pore Pressures and Displacements in Ramganga dam

by

V.M. Manglik*

R.C. Gupta**

Introduction

Ramganga River Project has created a reservoir in the Valley adjacent to Corbett National park in Uttar Pradesh for providing annual irrigation to 5.75 lakh hectares of land in Ganga Yamuna Doab and for generation of 451.8 million Units of power. The storage has been created by construction of two zoned earth and boulder fill dams (127.5 m high on the main river and 71.35 m high on a tributary to plug a saddle).

The Main Dam (Figure 1 & 2) rests on alternate bands of sand rock and clay shale of Middle Siwalik Age. The Valley is located in a high seismic zone. USBR type twin tube hydraulic piezometers (foundation and embankment types), electrical piezometers, combined vertical and horizontal settlement devices, stress meters, slope indicator devices and surface settlement monuments were provided in the body of the Ramganga Main Dam (Figure 1 & 2) to obtain measurements of seepage and construction pore pressures, settlements of dam foundations, settlements with-in the dam embankment, up stream—downstream horizontal strain within the dam, normal and horizontal stress distribution, horizontal displacements and surface movements, respectively.

The placement procedures and geotechnical properties of the different zones of embankment have been shown in Table-I, while the typical grain size distribution, typical *e*-log *P* curves and compaction curves in Figures 2(*c*), 3(*a*) & (*b*) and 3(*c*) & (*d*), respectively.

Pore Pressure

Pore pressures develop in an embankment as it compresses under its own weight during construction. When drainage of air and water is not possible, a pressure develops in pore air and pore water, opposing the externally applied stress. The interface between water and air in a partially saturated soil is curved; the water in the pores is stressed in tension and results in development of capillary stresses. The effect of this stress is to pull the soil particles together. Pore-water pressure is therefore sum total of pore-air pressure and capillary stresses (negative in nature). Pore-water pressure

---

*Chief Engineer, Ramganga River Project, Kalagarh, Uttar Pradesh, India.

**Executive Engineer, Test and Quality Control Division, Kalagarh, Uttar Pradesh, India.

Tne Paper is open for discussion till the end of October 1977.

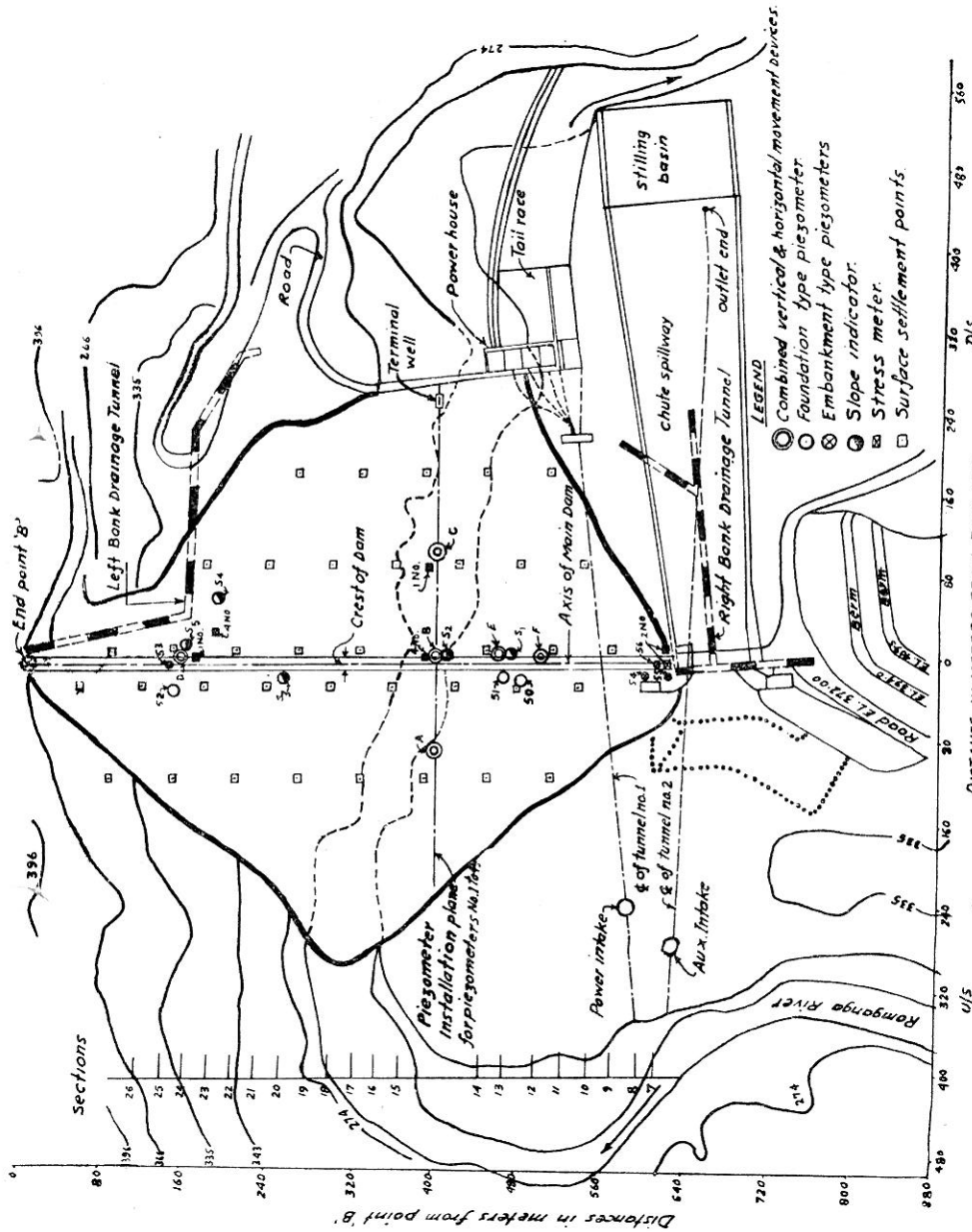

FIGURE 1. Instrumentation plan for Ramganga main dam

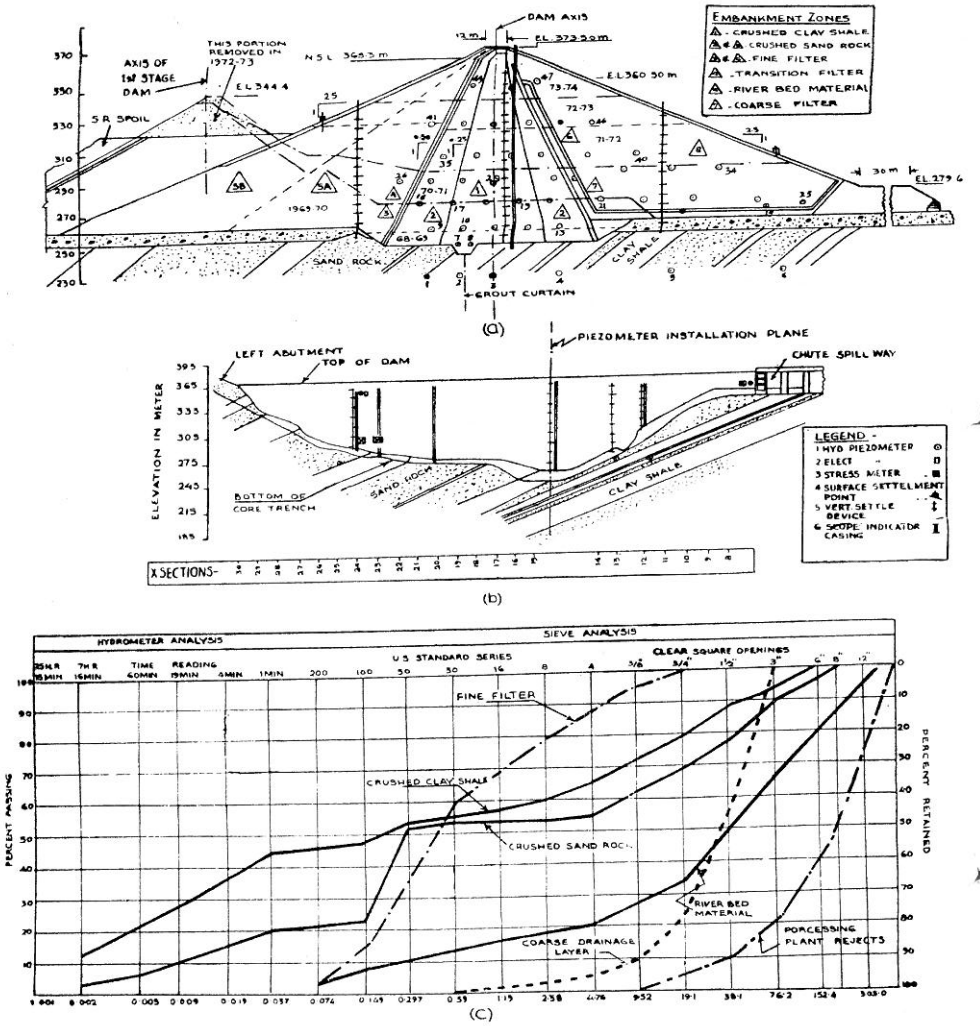

FIGURE 2. (*a*) **Typical cross section at deepest river bed**
(*b*) **Longitudinal cross section at dam axis**
(*c*) **Typical grain size distribution curves**

TABLE—I

S. No. Description	Estimated quantity of fill in Cu. m. $\times 10^6$	Average compacted dry density in kg/M³	Placement Moisture content in%	Compaction procedure	Geotechnical properties				
					K	c	ϕ	P.I.	γ_g
1. Zone-1, Crushed clay shale	1.37	2000	9 to 11	12 to 14 passes of Hyster compactor on every 150 mm thick layer	0.005	1.0	22°	6 to 14	2.70 to 2.73
2. Zone-2, Crushed sand rock	3720	1900	9 to 12	17 to 19 passes of Hyster compactor on every 300 mm thick layer	0.8 to 20	0.35	33°	Nil	2.66 to 2.69
3. Zone-8, Crushed Sand rock		1900	4 to 6	—do—but by 19-21 passes					
4. Zone-3&6, (-19)mm River Bed Material	1.200	1900	Natural Moisture Content	2 to 3 passes of 10 Tonne Vibratory Roller on every 600 mm thick layer	80 to 100	0.0	36°-35°	Nil	2.66 to 2.77
5. Zone-7, 5 mm to 75 mm River Bed Material		050				0.0	40°-45°		
6. Zone-5 (A), (—) 450 mm River Bed Material	1.200	2200			300 to 1000	0.0	38°-41°		
7. Zone-5 (B), 20 mm to 450 mm River Bed Material	2.120	1800			—	0.0	40°-45°		

Notes: (1) Crushed sand rock and crushed clay shale were so compacted that their (—) 4.8 mm faction attains atleast 100 percent standard Proctor's maximum dry density.

(2) River Bed Material was compacted to attain a density greater than 2160 kg/m². Filters were compacted to attain a density greater than their 70 percent relative Density.

(3) K=Coefficient of permeability in cm per second $\times 10^{-6}$, c=Cohesion in kg/cm², ϕ=Angle of Internal friction, $P.I.$=Plasticity Index, γ_g=Specific Gravity.

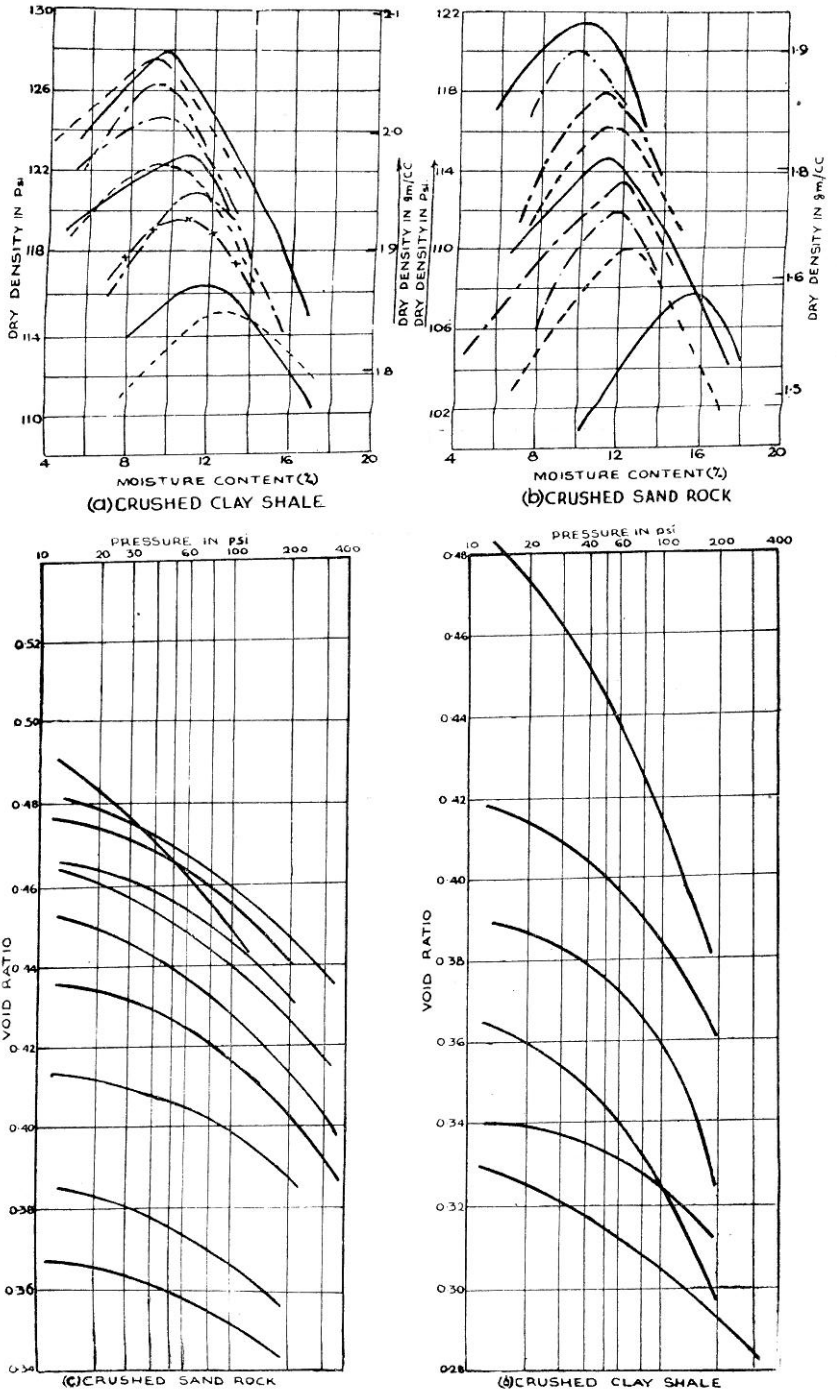

FIGURE 3. Compaction curves
(*a*) **for crushed clay shale**
(*b*) **for crushed sand rock**
and *e*-log *p* curves
(*c*) **for crushed sand rock**
(*d*) **for crushed clay shale**

is always lower than pore-air pressure and may even be held negative as a result of capillary stresses. Capillary stresses disappear upon saturation of soil mass.

Pore water pressures are also generated due to seepage of water from the reservoir through the dam embankment and foundation. Pore water pressure may also be generated due to seepage of water from the perched water table or aquifer present in the rocks.

Installations for Measurement of Pore Pressure

USBR-Type twin-tube hydraulic piezometers (43 embankment types and 6 foundation types) were installed in Ramganga Main Dam along one cross section of the embankment in the deepest river bed portion (Figure 1). The rocks at section 12, 13 and 24 were loose jointed and fissured and had taken heavy grout intake; therefore one foundation piezometer was installed in each of these bands. Three embankment type piezometers were installed at El.352 m in clay core along wall block no 102 of chute spillway to determine seepage pattern that would develop in the dam along the wall.

At Main Dam, five electrical piezometers alongwith hydraulic piezometer nos. 35, 36, 37, 38, & 53 were also installed, to confirm the reliability of measurements.

Design Factors for construction pore pressures

One dimensional consolidation tests were performed on samples of crushed clay shales (—4.80 mm) and of crushed sand rock (—4.80 mm) molded at (*i*) optimum + 2 per cent (*ii*) optimum + 1 per cent (*iii*) optimum (*iv*) optimum — 1 per cent moisture content and *e*-log *p* curves were drawn. Construction pore pressure (computed by Hilf's Formula) versus total stress curves (Figure 4) were then drawn. The contribution of capillary stresses was however ignored. On the basis of these curves following design values were adopted for stability analysis:

(*i*) for crushed clay shale $U_w = 0.5\sigma$

(*ii*) for crushed sand rock $U_w = 0.25\sigma$

(*iii*) for crushed sand rock $U_w = 0.125\sigma$ in zone-8

where σ is total stress.

Pore Pressure Data

Pore water pressure [as sum total of observed pore pressure at the tip (in meter head of water) and the respective tip elevation in m] versus time plots are shown in Figure 5 and 6, while observed pore water pressure (in kg/cm²) versus total overburden stress (kg/cm²) in Figure 7. Series of diagrams of pore pressure contours at deepest river bed section of Main Dam shown in Figure 8 & 9, include several dates during construction period and first two years of reservoir filling.

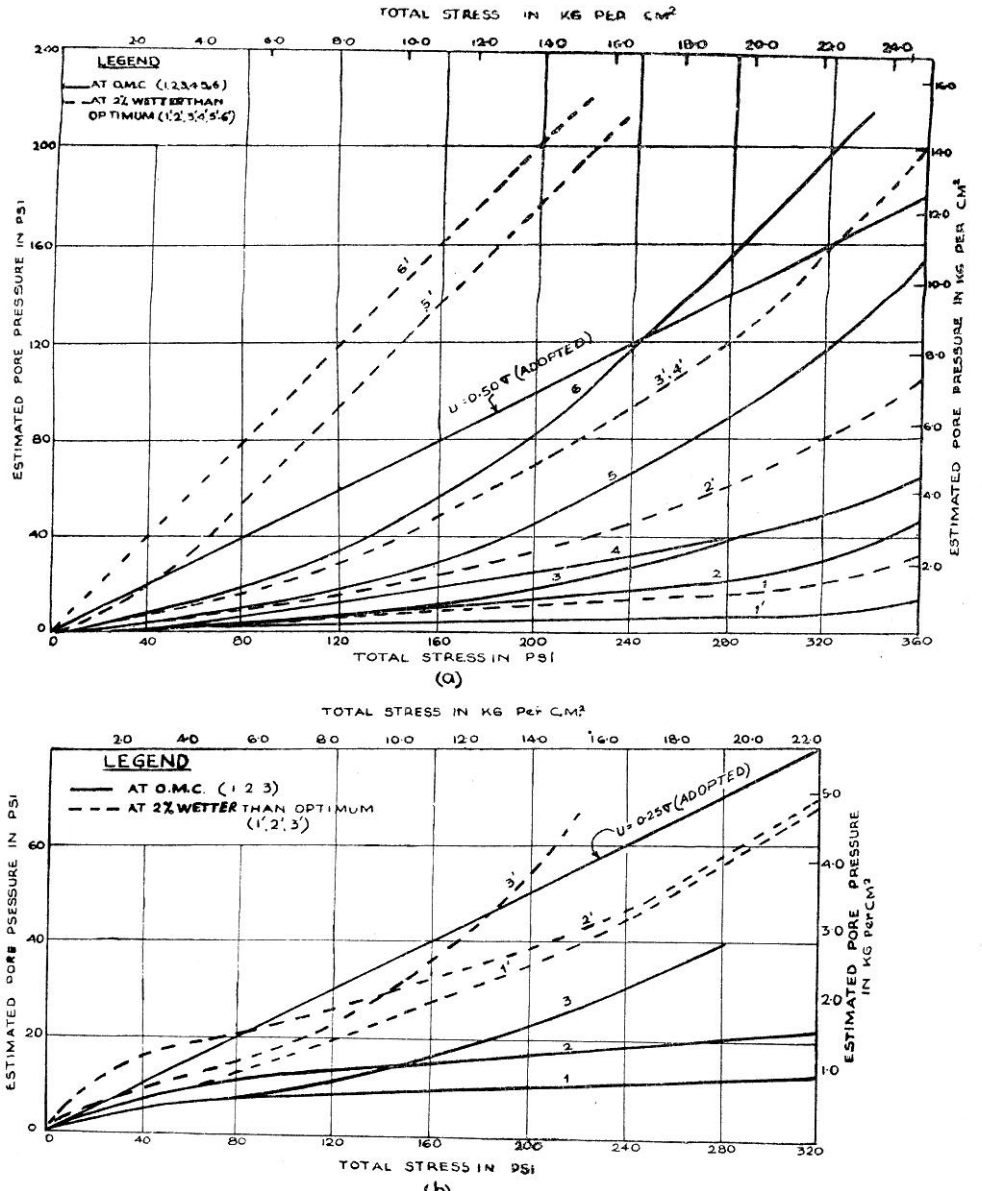

FIGURE 4. Estimated construction pore pressures vs total stress curves for
(*a*) compacted crushed clay shale
(*b*) compacted crushed sand rock

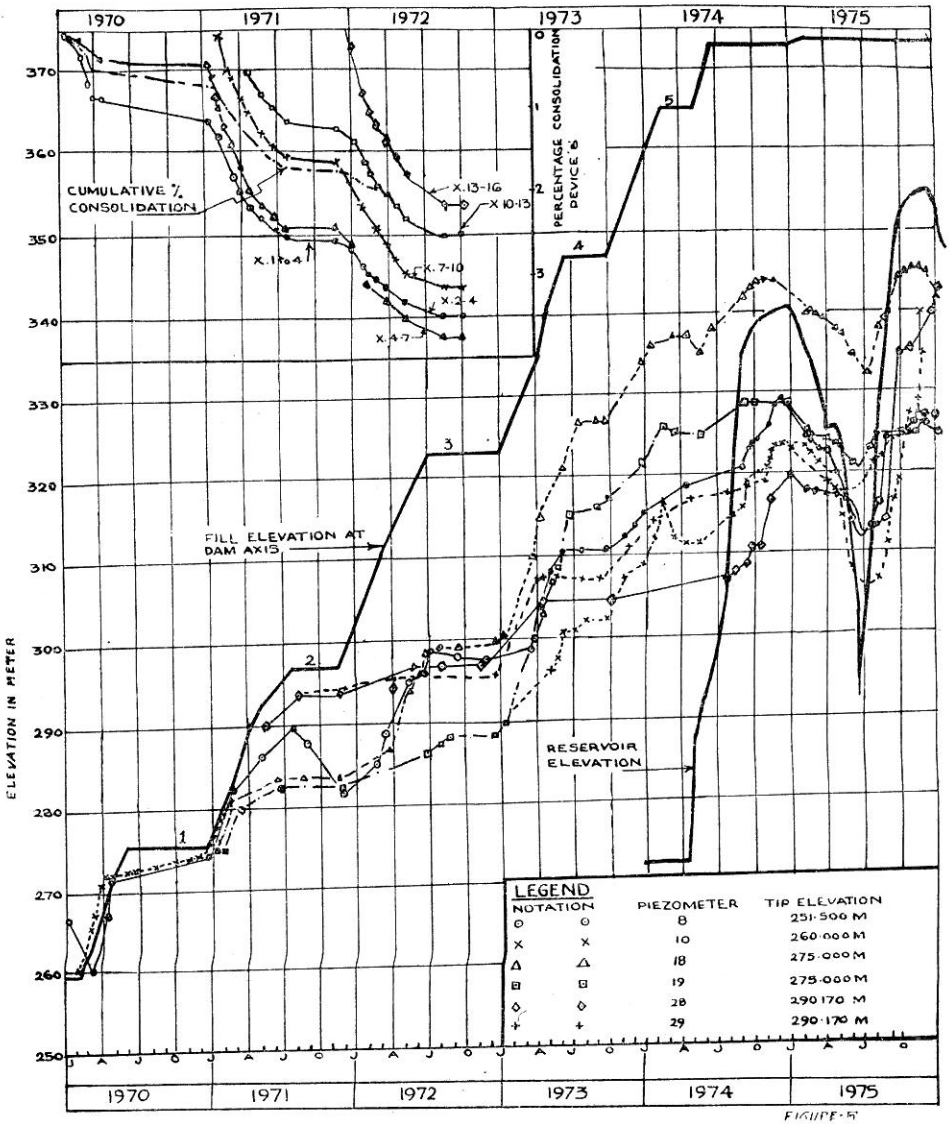

FIGURE 5. Observed pore pressures and percent consolidation in clay core (obtained from device 'B')

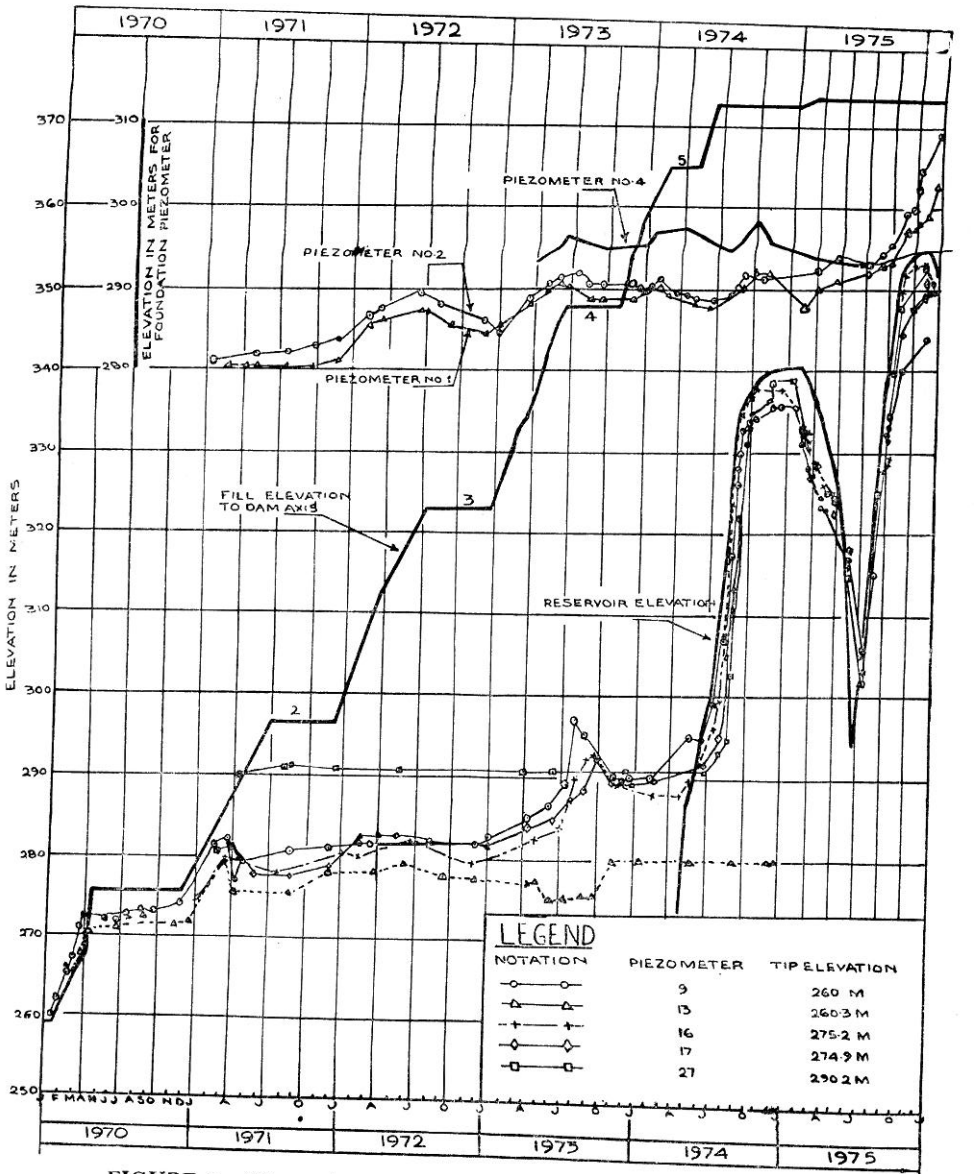

FIGURE 6. Observed pore pressures in crushed sand rock (zone-2) and Foundation rocks

Construction pore pressures

(*a*) Construction pore pressures in clay core closely paralleled the progress of placing operations (Figure 5). In the initial period, the intensity of pore pressures recorded by piezometers nos 8 and 10 is on average, 0.43σ while by piezometers nos 18, 19, 28 and 29 about 0.2σ. The variation in intensities of pore pressures appears to be due to change in moisture content of the clay fill at respective tip location. The fill in the core after having been laid upto El 258 m by June '69, was covered by river bed material to allow the river to flow during monsoon season on the river bed so prepared. Therefore clay and sand rock fills in core were wetted by the river water and this resulted increase in moisture content and intensities of construction pore pressures in piezometer no. 8.

When a layer of soil is near optimum and the layer below it, is a fairly saturated soil, it shall induce sucking of moisture from the lower wet layer. Added weight of the fill shall compress the soil and the pressure developed in the pore fluid will tend to squeeze out the pore-water to the areas, where soil is comparatively drier. Although clay fill near piezometer no. 10 (at El 260 m) was placed at moisture near optimum, it may have been got wetted by the above two actions taking place in the lower wet layer. This action was probably responsible for development of high intensities of construction pore pressures (upto 0.43σ) in clay fill (in the vicinity of piezometer no. 10). Clay fill near piezometer nos. 18 and 19 (located at El 275 m) were not affected by such phenomenon and therefore remained at placement moisture content (near optimum) and recorded low intensities of construction pore pressures (in the range of 0.2σ).

(*b*) Piezometers in clay core recorded rise in the intensities of pore pressures during several shut down periods of placing operations (Figures 5 & 7). It is indicative of gradual compression of clay layers due to delayed lateral transfer of superimposed loads.

During certain shutdown periods of placing operations (Figure 5 &7), the piezometers have recorded fall in the intensity of construction pore pressures, indicating some drainage of air at higher intensities of pore pressures when a drainage path was established.

(*c*) The ratio of construction pore pressures with respect to total stress at the end of construction is on average 0.3 for zone-1 clay core (maximum value-0.32), 0.10 (maximum value 0.15) for zone-2 crushed sand rock & nil (maximum value 0.1 for only few tips at lowest elevations where fill was placed near optimum) for zone-8 crushed sand rock.

(*d*) Initially, construction pore pressure zone-2 crushed sand rock was about 0.4σ (Figures 6 & 7); no significant rise in the intensity of pore pressure occurred later indicating significant dissipation of pore pressure due to high permeability of crushed sand rock (0.8 to 20×10^{-6} cm/sec).

(*e*) Negative pore pressures have been observed in clay core at elevations

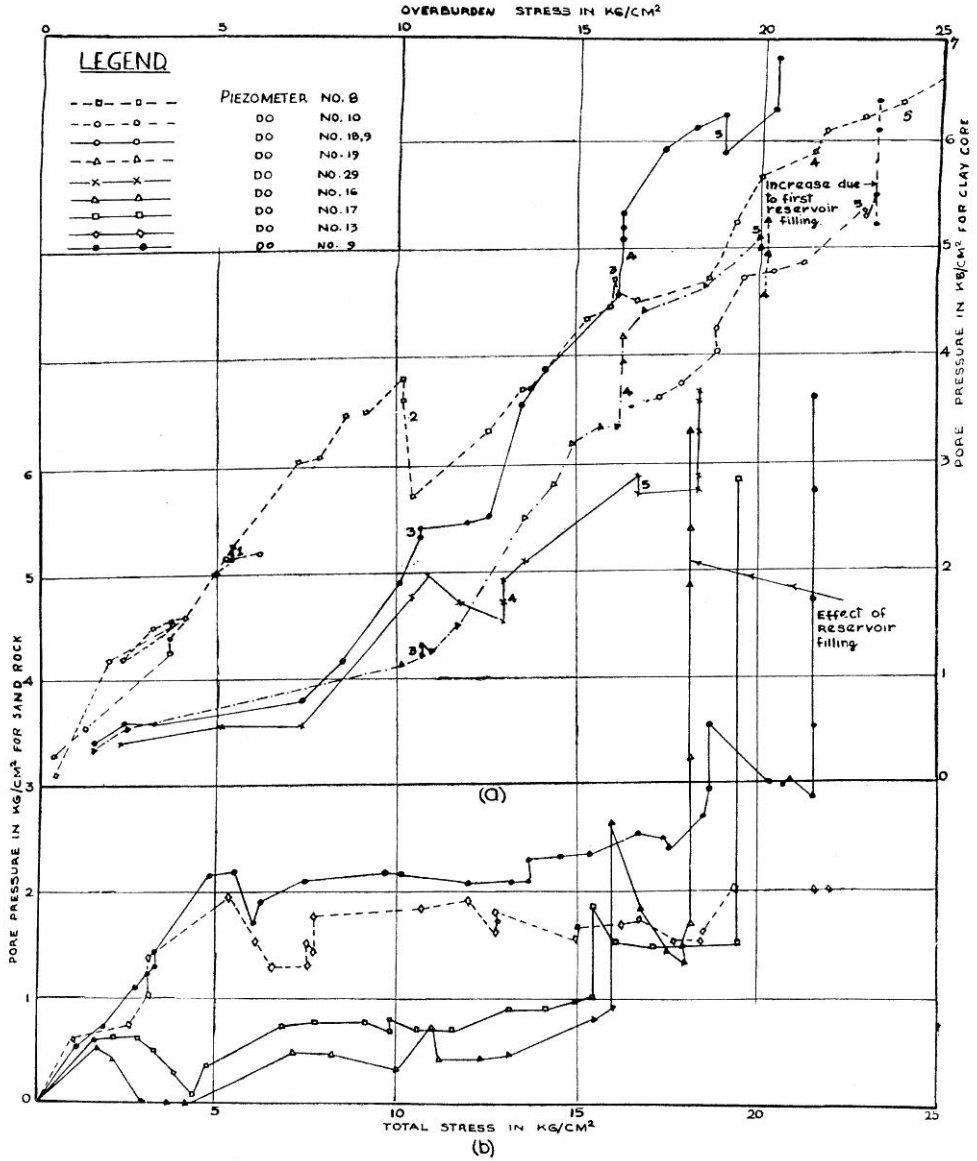

FIGURE 7. Computed total stress vs observed pore pressure curves for
(*a*) clay core
(*b*) sand rock zone-2

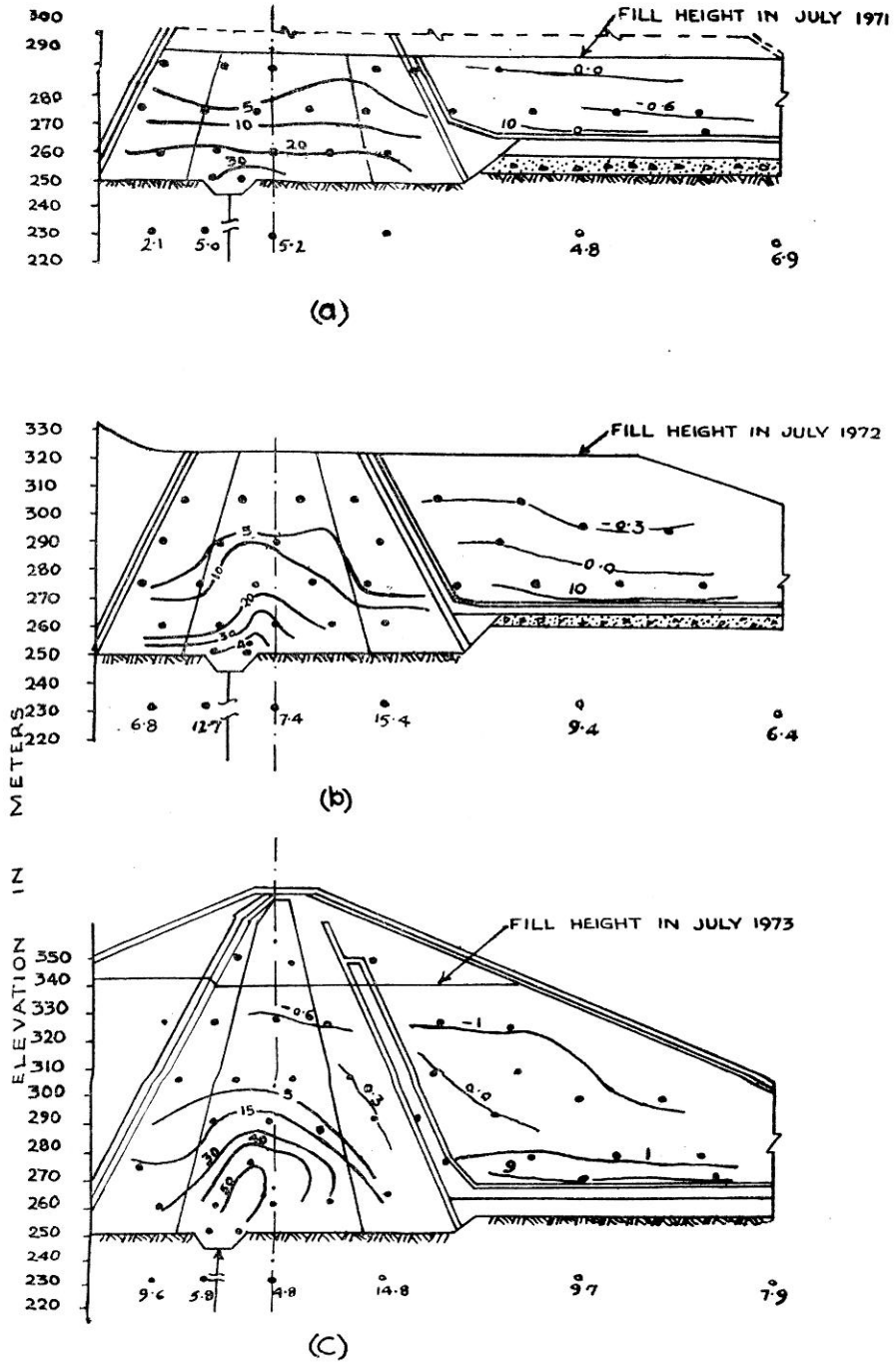

FIGURE 8. Pore Pressure contours

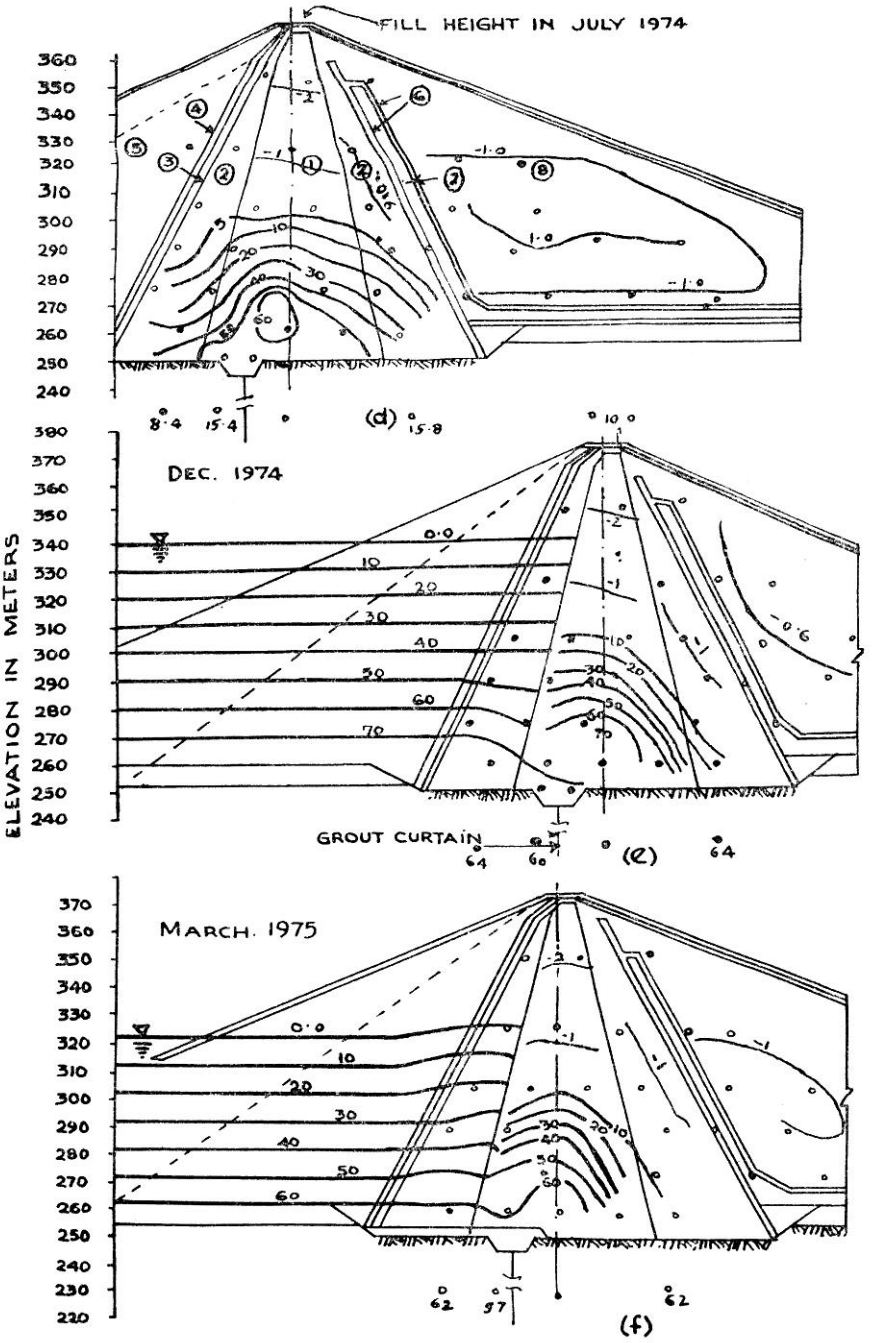

FIGURE 8. Pore Pressure contours

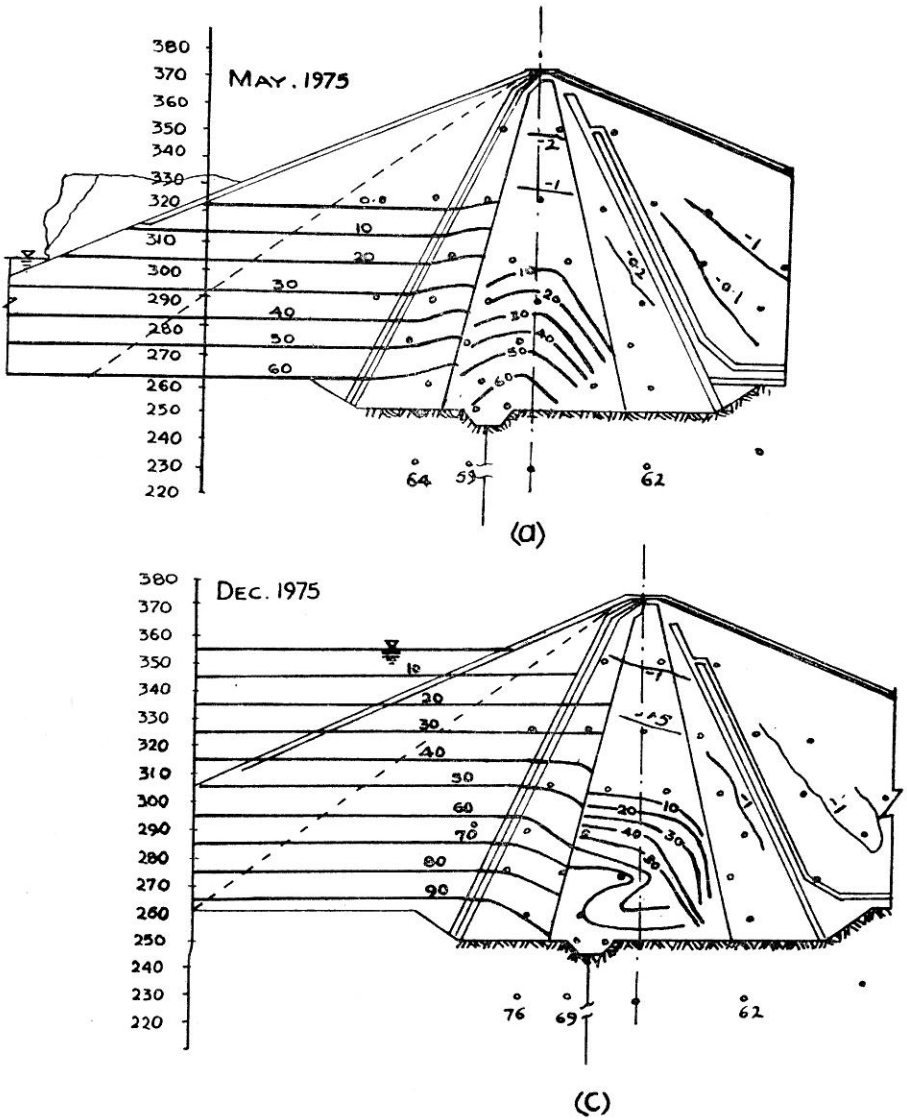

FIGURE 9. Pore Pressure contours

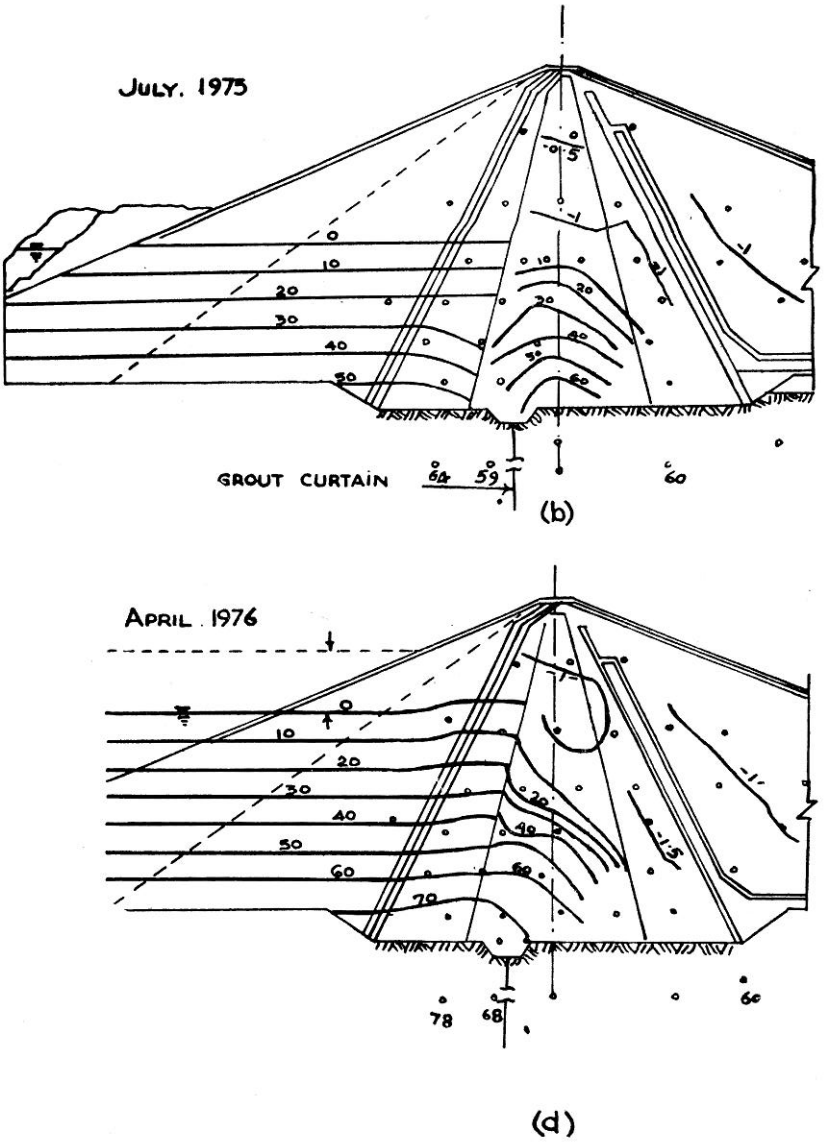

FIGURE 9. Pore Pressure contours

higher than 305 m (Figures 8 & 9), indicating that intensity of capillary stress is more than pore-air pressure and pore-water has been even held negative. Clay for zone-1 upto elevation 305 m was borrowed from chute spillway excavations, while above El 305 m, from left abutment borrow area (downstream of Main Dam). Plasticity Index for clay borrowed from chute spillway excavations varied from 4 to 10, while for left abutment excavations from 8 to 14; this may have also accounted for development of high capillary stresses at higher elevations.

Negative pore pressures were also observed in zone-8 crushed sandrock fill laid at moisture content of 4 to 6 per cent only. When the existing water content of a sample is less than its capacity, a water deficiency exists (known as water thirst). Higher water deficiency will be responsible for higher tendency to generate negative pore pressures (Lambe, 1961).

(*f*) Pore pressure contours are parallel in July '71 (Figure 8) which indicates development of nearly the same intensity of pressures initially both in zone-1 clay and zone-2 crushed sandrock (both laid near optimum). However these became significantly convex upwards in July '72 & July '73 (Figure 8*b* & *c*), indicating drainage of air from zone-2 crushed sand rock, resulting in dissipation of pore pressures. The pore pressue contours therefore reflect the placement condition of core and the influence of drainage.

Pore pressure contour of highest intensity was found in central portion of clay core near cut-off trench, (Figure 8 *d*) where possibility of drainage was the least.

Changes in intensities of pore pressures during reservoir filling

(*a*) The increase in pore pressues in zone-5 (river bed material) is proportional to the rise in reservoir level (Figures 8 and 9). The pore pressures dissipate as the reservoir is depleted but not as speedily as the reservoir.

(*b*) The pore pressures in sand rock zone-2 rise as rapidly as the reservoir level (Figure 6), indicating the effect of easy seepage of reservoir water in sandrock zones. The dissipation of pore pressures with fall in reservoir level in sand rock zone-2 (*a*), varies from 25 to 52 per cent of the maximum pore pressures reached during steady reservoir condition, where as in design, no dissipation of pore pressure has been assumed. The behaviour is on the safe side.

The configuaration of pore pressures (Figure 8 and 9) demonstrates drawdown curves in sandrock zone-2*a*. Reservoir water from upstream pervious zone-5 was not drained off immediately due to presence of crushed sand rock spoil on upstream slope (left in this portion as waste), even though reservoir was depleted to El 300 m in May '75 and this lead to configuration of pore pressures as shown in Figure 9 *a*.

Residual seepage pore pressures in sand rock zone-2 (*a*) were completely dissipated in July '75 (Figure 9 *b*).

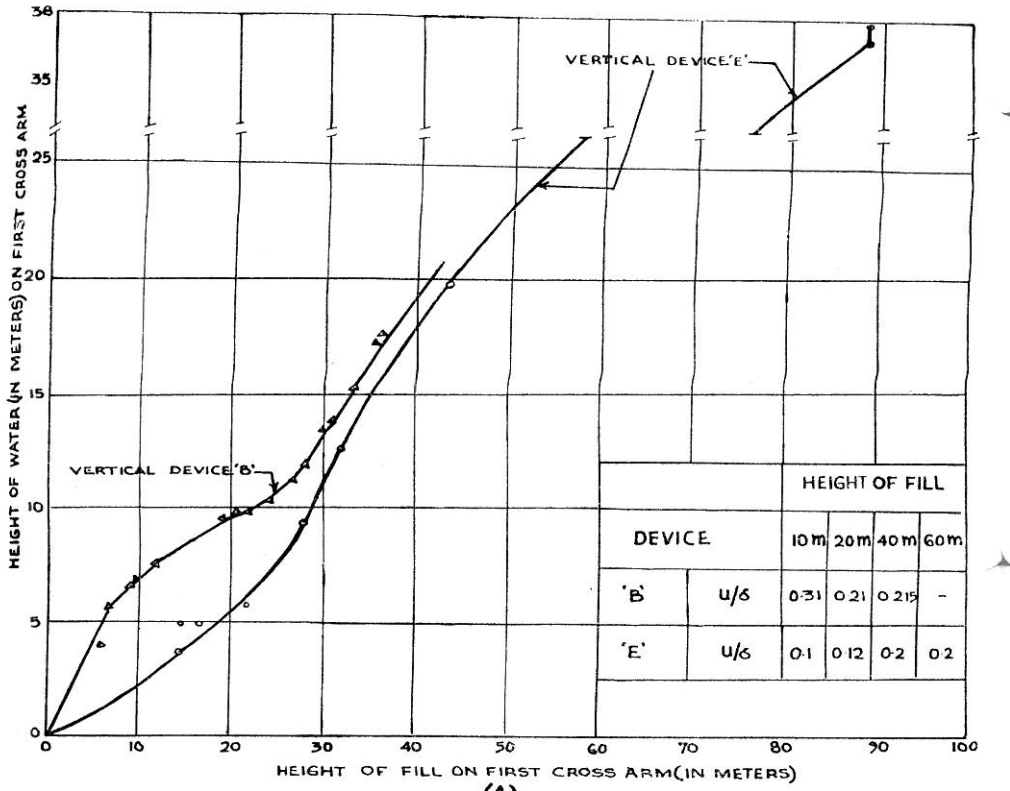

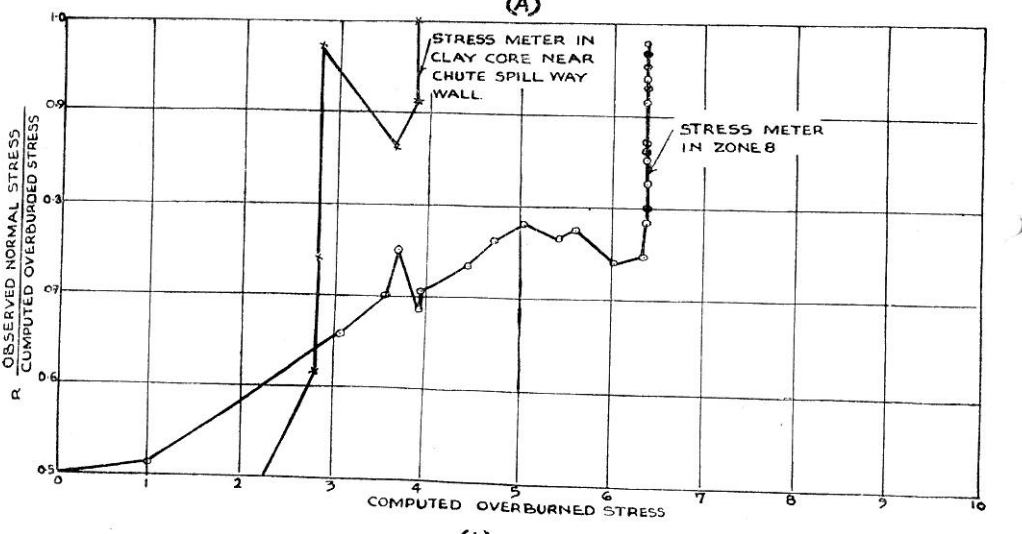

FIGURE 10. (*a*) Water level in cross arm telescoping pipes
(*b*) observed normal stress curves in zone-8 and clay core near chute spillway

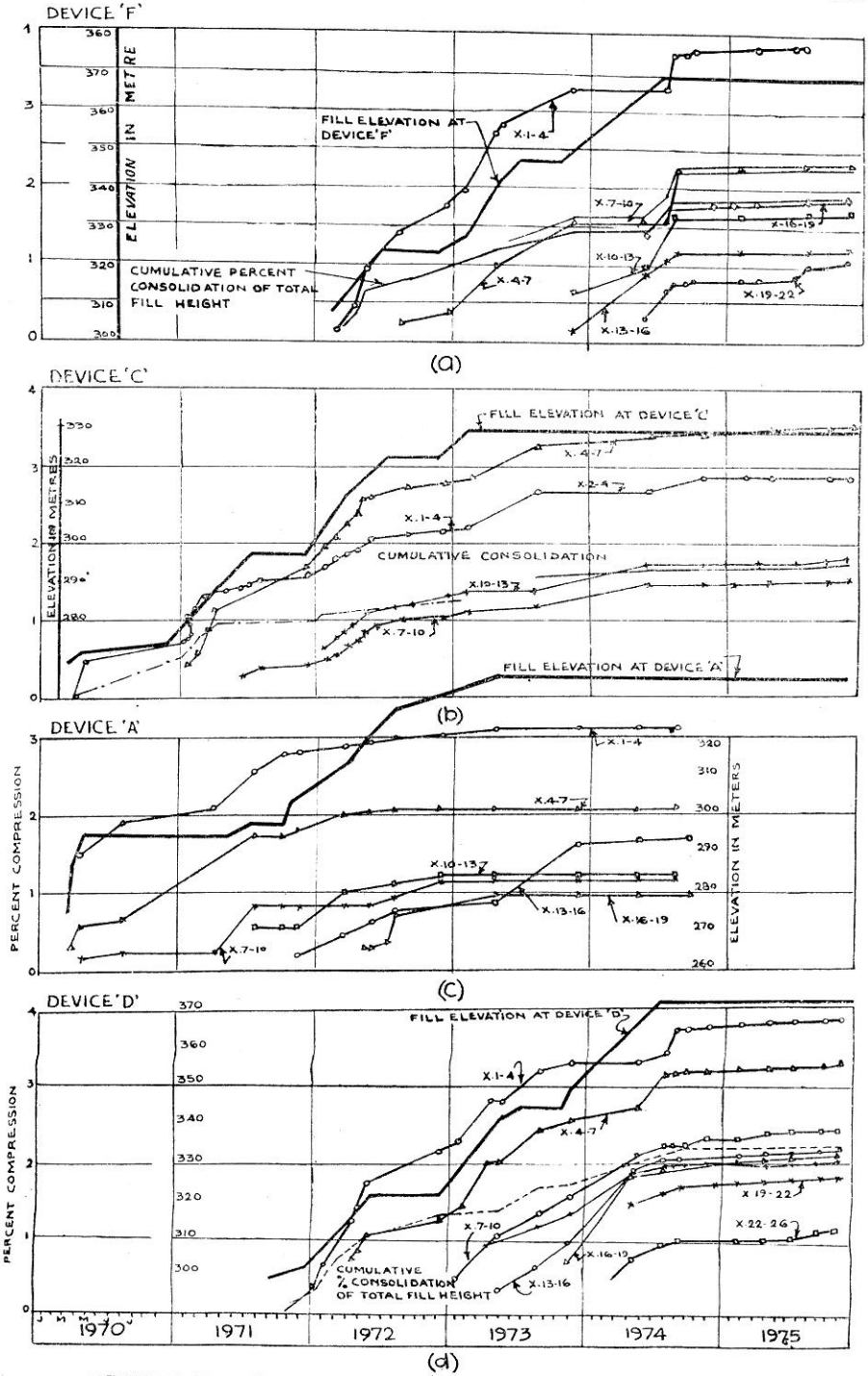

FIGURE 11. Time-percent compression curves obtained from vertical settlement Devices F, C, A and D.

(*c*) The increase in intensities of pore pressures in clay core (below El 305) of the order of 9 m of water head was recorded during first reservoir filling (Figure 5). When first filled, the reservoir imposed a load on the structure which decreased shear stresses and raised vertical effective stresses in upstream zones of low permeability to their maximum values. The increase is pore pressures was greater in up stream portion of the clay core indicating greater influence of reservoir load upstream half of the embankment. This load produced additional compression of clay core (Figures 11 and 12) which resulted in increase in the intensities of pore pressures.

Penetration of seepage during first filling of reservoir, increasing the degree of saturation of clay core had not taken place as piezometer no 18 continued to record hydrostatic head above the maximum reservoir elevation (Figure 5) and negative pore pressures which disappear on saturation continued to occur in clay core over elevation 305 m. The configuration of pore pressures (Figure 8 *e*) also do not reflect penetration of seepage in clay core except in lowest portion of the upstream half of the core.

(*d*) Dissipation of construction pore pressures during depletion of reservoir (between 24-12-74 to 20-6-75) in the order of 14 m of water head took place (figure 5) in clay core. Dissipation of pore pressures produced a corresponding increase of the stress in the soil skeleton. Consolidation accompanying the increase in effective stress occurred as a process of recompression (Figures 11 and 12), since intergranular pressures reached their maximum at the first filling of reservoir.

(*e*) Increase in the intensities of pore pressures (in piezometer nos 8, 10, 18, 19, 28 and 29 being 14 m, 15 m, 13 m, 3 m, 32 m, and 20 m) in clay core was again recorded during reservoir filling in year 1975 (Figure 5). The configuration of pore pressures (Figure 9*c*) reflect penetration of seepage in upstream half of the core increasing the degree of saturation. The seepage has however not crossed clay as it has not entered in zone-2*B* (where no increase in pore pressures has been observed).

(*f*) Figures 9(*d*) shows the configuration of pore pressures during depletion of reservoir in year 1976. It can be seen that dissipation of pore pressures is taking place both in clay core and sand rock zone-2*b*. The flownet in clay core shall fully develop when the reservoir seepage has entered in all parts of clay core and it appears to have fairly developed below El 305 m.

(*g*) No change in the intensities of pore pressures has been observed in crushed sandrock zone-8 and in chimney filter system (Figure 8 and 9) indicating that the seepage has not entered these zones.

Foundation Piezometers

Holes (42 m to 51 m deep) were drilled in the rock for installation of foundation piezometers, when embankment elevation had reached El 276 m. After installation of the tips, hole was backfilled with clay slurry. The initial readings observed, were found generally in the range of the depth of hole; it

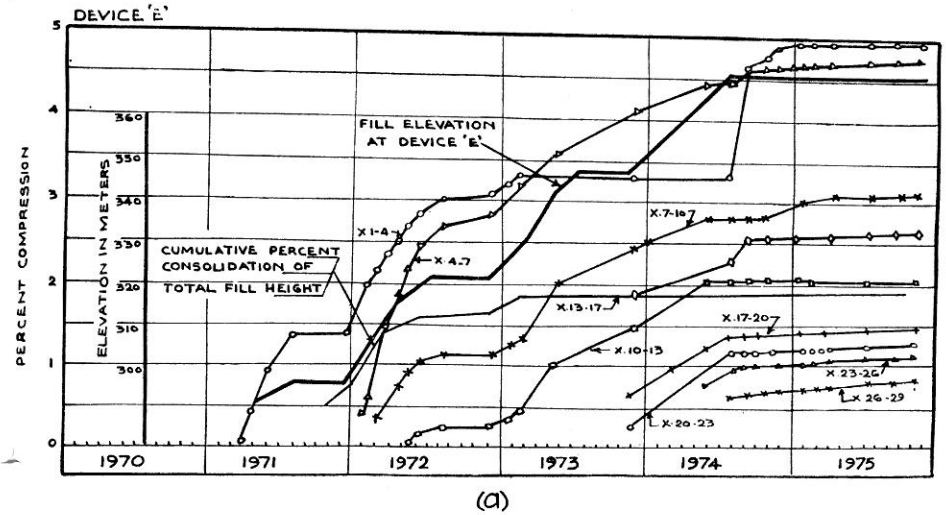

(a)

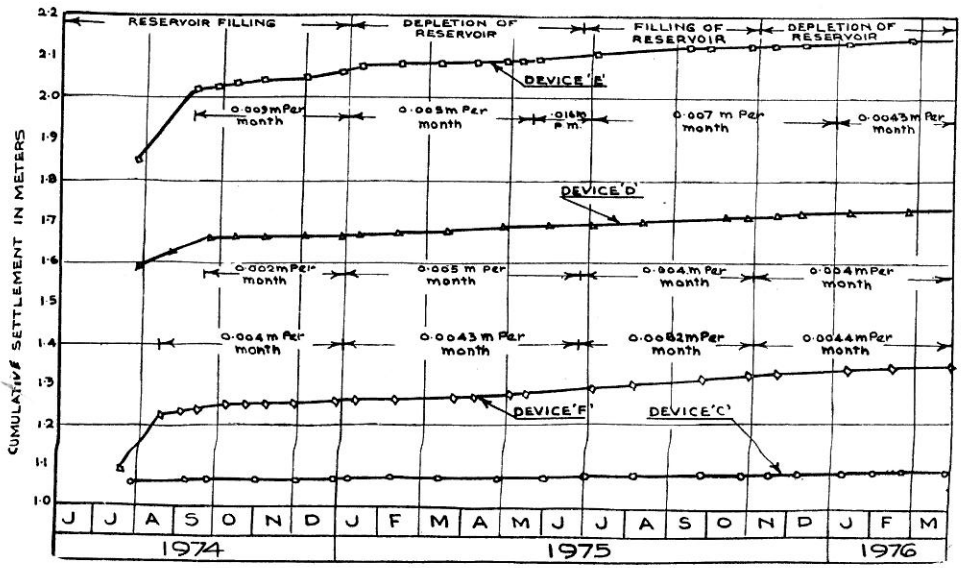

(b)

FIGURE 12. (*a*) **Time percent settlement curves obtained from vertical settlement dervice E**
(*b*) **Cumulative post construction settlement**

was therefore considered that these readings are due to hydrostatic head exerted by water present in clay slurry (Figure 6) and that all subsequent readings if deducted by the initial readings would give the value of foundation pore pressure [shown in Figures 8 (*a*), 8 (*b*) and 8 (*c*)] developing due to recompression of rocks under the superimposed loads. The presence of ground water in rock was not noticed during drilling of holes as the holes were found dry. The intensities of construction pore pressures in the rocks range from 0.34 to 1.56 kg/cm^2 when the superimposed loads were in the order of 26 to 30 kg/cm^2; these are as expected of very low order due to their high densities. In 1974, the intensities of foundation construction pore pressures increased by about 0.3 kg/cm^2 due to reservoir load on upstream slope of the dam. All foundation piezometers (both at upstream and down stream of grout curtain) showed that reservoir seepage could not penetrate in the rocks (Figure 6).

During reservoir filling in year 1975, the reservoir seepage penetrated in the rocks upto locations of foundation peizometer nos 1 and 2 and produced rise in the intensities of pore pressures by 15.6 m in piezometer no. 1 and 10.3 m in piezometer no. 2 (Figure 6). However, insignificant increase was recorded by piezometer no. 4 (placed downstream of grout curtain) which shows that grout curtain is effectively functioning for providing an impervious barrier. To show the effect of reservoir seepage, the intensity of foundation pore pressure as observed (without deducting the initial reading) has been written in figures 8 (*e*), 8 (*f*) and 9.

Water column in Telescoping Pipes

The moisture of the soil is squeezed out into the cross arm telescoping pipes due to compression of the soil mass even in partially saturated soil. The increase in the level of water in telescoping pipes takes place with increase in percent compression and fill height (Figure 10 *b*). The standing column of water in the pipe would obviously be equal to the pore pressures developing in the adjoining soil mass. However there can be some time lag between the increase in pore pressures in the soil and corresponding increase in height of water column in the pipe. It can be seen from this figure that pore pressure results obtained from reading of height of water column in the pipes are quite close with the results obtained from twin tube hydraulic piezometers.

Compressive Characteristics of Main Dam

Vertical Device nos *A*, *B* and *C* were installed in Main Dam in its upstream pervious shell, clay core and downstream outer shell, respectively, to determine the compression characteristics of the dam foundation and the dam fill at the deepest river bed section (Figure 2 *a*). Vertical devices *E* and *F* were also provided in clay core near steep right abutment, while device *D* at steep left abutment, to carefully observe the behaviour of clay core near steep abutments of Main Dam (Figure 2 *b*).

Nature of Vertical Strain

The observed shortening of the vertical distance between two consecutive cross arms in a telescoping pipe system is caused by deformation of three types: primary consolidation, secondary compression and shear strain (Gould-1954).

"Primary Consolidation" is a decrease in the volume of the soil mass with strain in vertical direction only.

"Secondary Compression" is an one-dimensional Volume decrease with complete lateral restraint which continues with time under a constant effective stress.

"Shear Strain" is a change in shape, but not in volume, of the soil mass caused by a difference in principal stresses.

Time-Percent Consolidation Curves

Time percent consolidation curves, derived from the measured settlement of cross arms are shown in Figures 5, 11 and 12. For this analysis, each telescoping pipe system was separated into consecutive groups of three 3 m vertical intervals and the shortening of these 9 m lifts determined. The cumulative shortening of lift upto a particular date was converted to consolidation in percent of total initial height of the vertical interval.

Following compression characteristics were noticed:

The dead load of the fill was transferred immediately to the grain skeleton as overburden was added during construction. Observed consolidation of these materials closely paralleled the progress of placing operations at the location of the telescoping pipe system and the primary consolidation under the fills weight ended with completion of the embankment. The abrupt change in the slope of consolidation curves at the end of construction represents the change from primary to secondary compression.

During shut down periods of year 1970 and 1971, percent compression in all the 9 m vertical lifts of clay core showed increase alongwith increase in the intensity of pore pressure, this may indicate additional compression with time due to delayed lateral transfer of load. Delayed lateral transfer of load has also been indicated by stress meters (explained subsequently in this paper).

It can be seen from the Table II that the coefficient of volume compressibility (ratio of vertical strain to the corresponding increase of effective stress) is the maximum for clayshale, followed by crushed sand rock. It is the least for well compacted river bed material.

Cumulative percent consolidation of total fill height at respective location of cross arm installations '*D*', '*E*' and '*F*' (so also percent consolidation of each 9 m vertical lift) is found to increase after completion of the Main Dam (Figures 11 and 12). Increase in its value during reservoir filling in 1974 and 1975 is obviously due to added weight imposed by reservoir on the upstream sloping face of the dam, while in June '75 (by which time the reservoir had been depleted to El 293.1 m) due to dissipation of pore pressures producing a corresponding increase of the effective stress in the soil skeleton.

However a significant increase in percent consolidation between June '74 (when Main Dam was completed) and August 1974 in Device '*D*', '*E*', '*F*' (Figures 11 and 12 and table II) appears to be due to delayed load transfer of superimposed loads. Cumulative post construction consolidation

TABLE—II

S.No.	*Vertical Device*	*Percent consolidation of the lowest 9 m vertical lift at effective stress of*		
		6 kg/cm²	*10 kg/cm²*	*15 kg/cm²*
1.	Device 'A' in Zone-5, River Bed Material	1.50	2.89	3.12
2.	Device 'C' in Zone-8, crushed Sand rock	1.96	2.90	3.40 at 11.5 kg/cm²
3.	Device 'B' in Clay core	2.12	3.20	Device choked
4.	Device 'D' in Clay core	1.99	3.27	3.70 at 13.8 kg/cm²
5.	Device 'E' in Clay core	2.37	3.26	4.60
6.	Device 'F' in Clay core	1.90	3.29	3.74 at 12.2 kg/cm²

(after August'74) observed upto Dec. 75, has been found to be 0.99 percent (0.11 m), 0.04 percent (0.127 m), 0.11 percent (0.111 m) of original height in Device '*D*', '*E*' and '*F*', respectively. The average rate of increase in post construction settlement in clay core is 0.004 m per month (Figure 12 *b*). Cumulative post construction consolidation of the twenty five USBR Dams generally has been less than 0.2 per cent of the original height in three years and 0.4 percent in periods as long as 14 years (Gould–1954).

Post construction consolidation in Device '*C*' located in crushed sand rock zone—8 is quite low as expected. The rate of increase in post construction settlement in this zone (Figure 12 *b*) is only 0.002 m per month.

Significant increase in percent compression (maximum value 0.40 per cent) of individual 9 m vertical at location of vertical device '*A*' and '*C*' was observed (Figure 11), even after the date of completion of full embankment elevation (399.3 m and 332.2 m, respectively) along these installations. This is obviously due to dispersal of superimposed loads of embankment placed in central zone (above the embankment elevation along these installations) resulting in increase in total stress. In part, the increase can be due to contribution of shear deformation which is most liable to occur where the lateral restraint is the least (i.e. near the outer slopes). The increase in total stress (Figure 14 *b*) in outer zones due to dispersal of loads of central embankment was calculated on the basis of charts published by Osterberg (1957)

Field compression Curves

Vertical effective stresses along a telescoping pipe system in an embankment were obtained by subtracting observed pore pressure from the dead load stresses of the fill (Figure 13). Vertical stress was plotted in the horizontal direction, scaled in units of meter of water pressure to conform directly to piezometer reading. The heavy slanting lines represent the distribution of total vertical stress (represented by abscissas between the axis and slant line) along the telescoping pipe system at various dates. These lines intersect the vertical axis at the surface of the fill on the date specified. The pore pressures observed at a particular date were also plotted horizontally in units of meter of water pressures at the elevations of piezometers. Abscissa between the total stress line and the pore pressure curve for a particuler date are effective vertical stresses in the soil skeleton.

Early in the construction, when the surface of the fill is broad and flat (i.e. when the width of fill surface is atleast twice the height of dam), the total stress distribution is triangular at any depth equal to the depth of overburden. Devices *B, C, D* and *E* were located on the edge of crest of Main Dam, where the actual stress at completion of dam is reported to range from 86 to 91 percent of the overburden (Gould 1964). The distribution of total vertical stresses along a telescoping pipe system at completion of construction was therefore assumed to be 90 percent of the overburden stress. The distribution of total stress in middle stages of construction (i.e. at the elevation of the fill when fill surface is less than twice the height of cross arm installation) was interpolated between the simple hydrostatic condition and the stress profile estimated for completion.

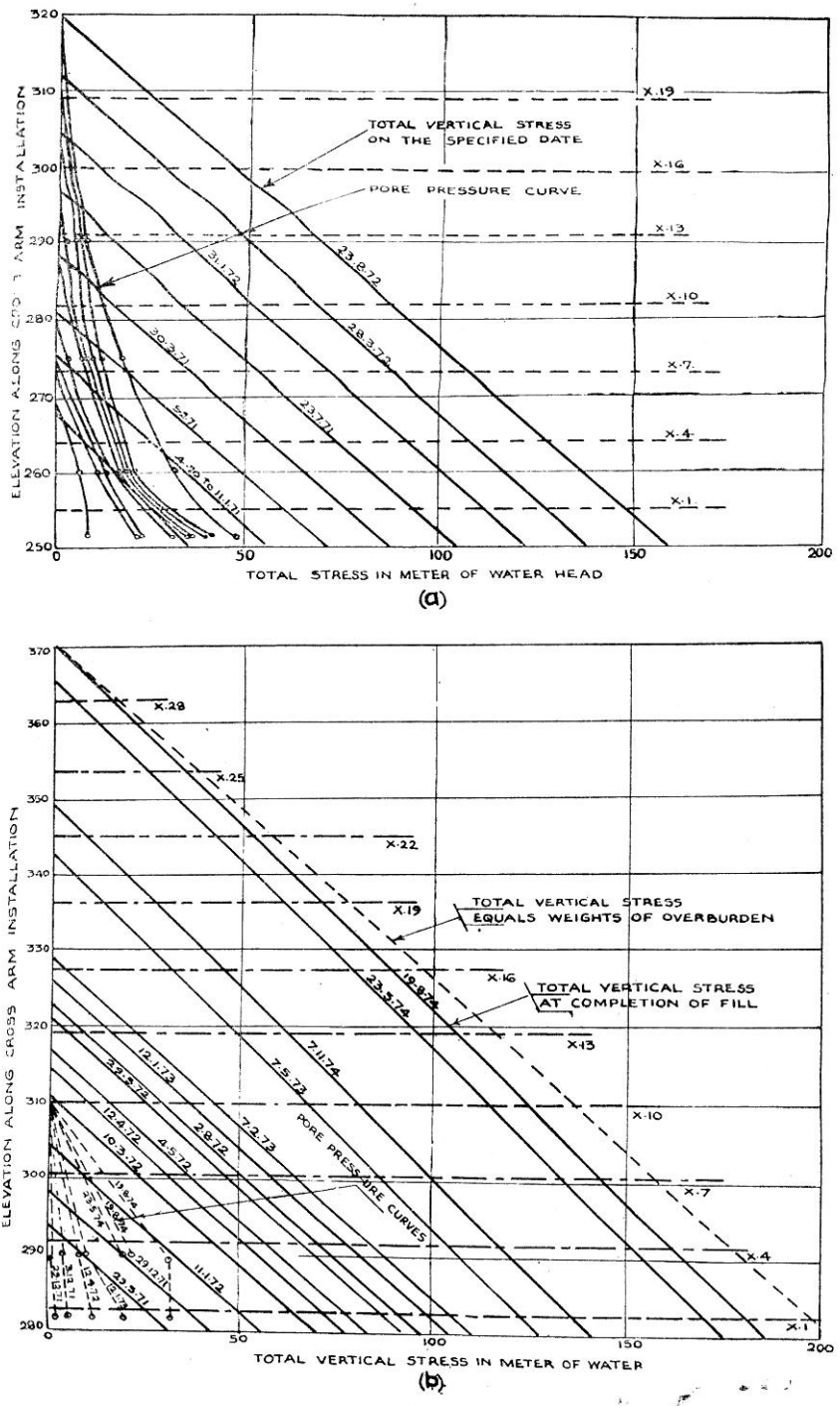

FIGURE 13. Distribution of vertical stress
(*a*) along vertical settlement device B in clay core
(*b*) along vertical settlement device in E clay core

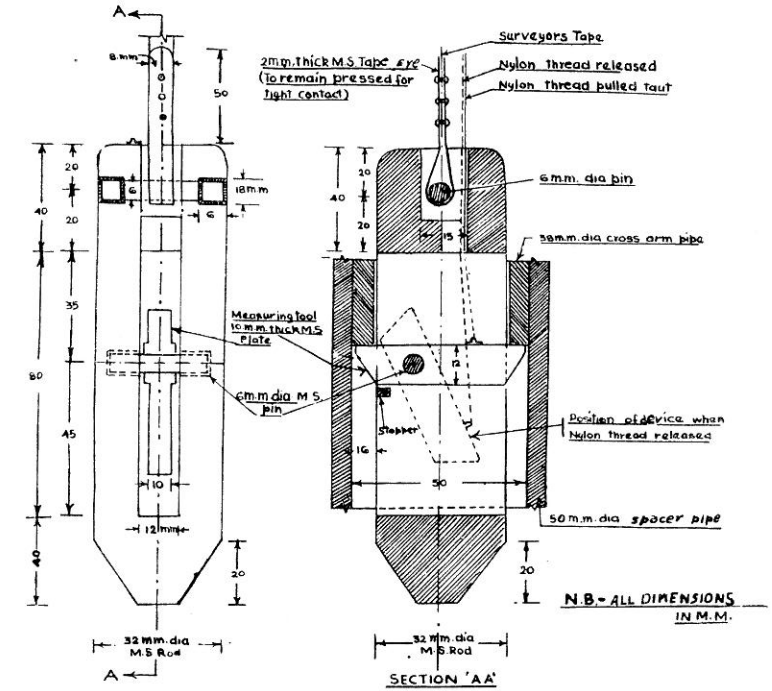

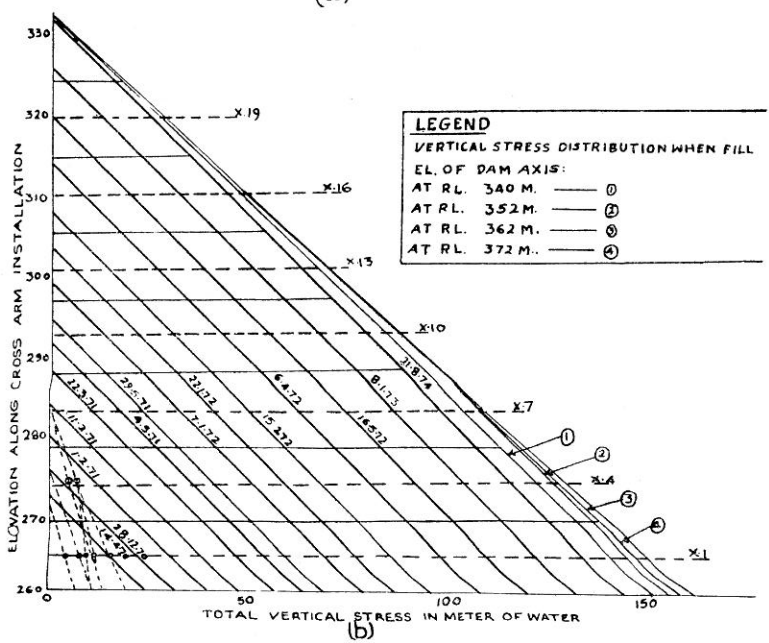

FIGURE 14. (*a*) **Details of measuring Torpedo for telescopic pipe system**
(*b*) **Distribution of vertical stress along vertical settlement device C**

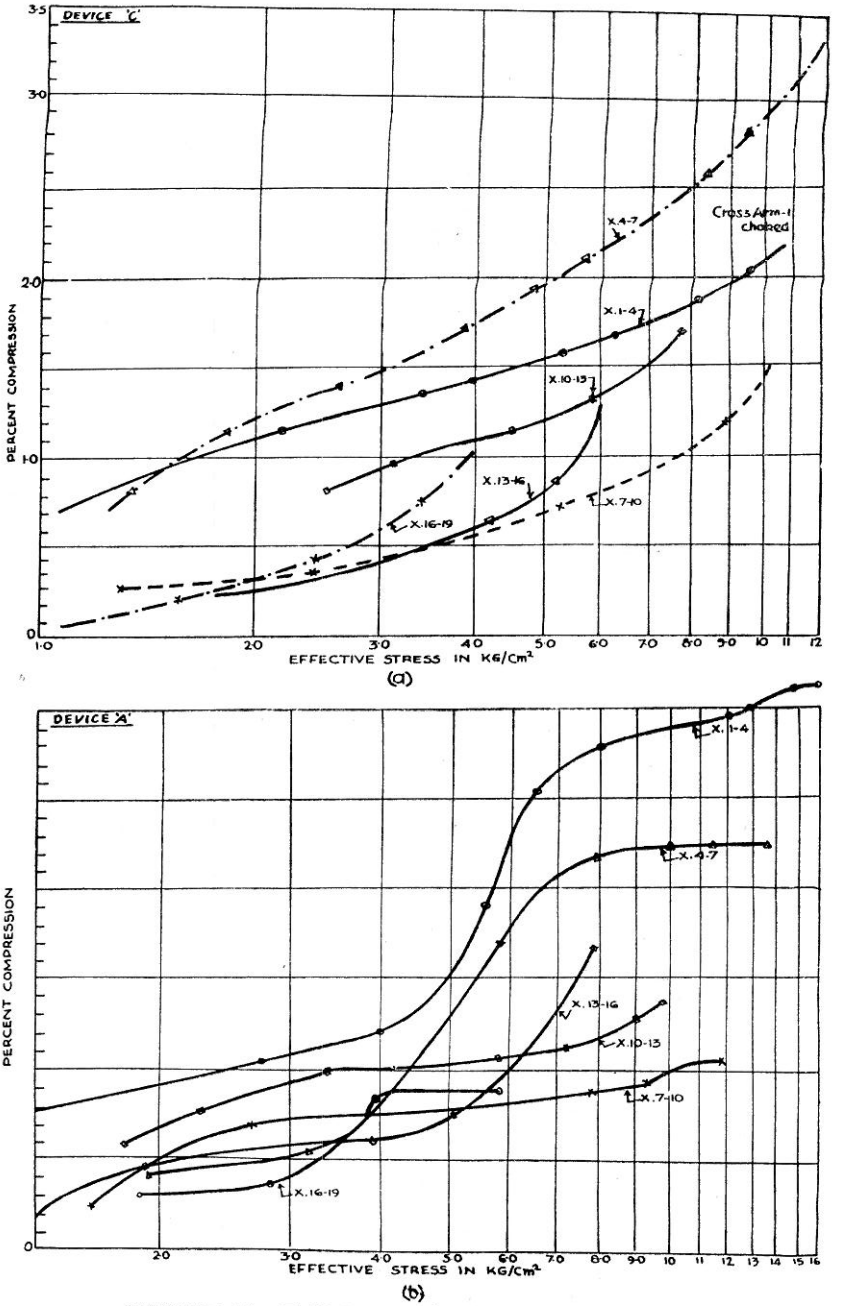

FIGURE 15. Field Compression Curves obtained from
(*a*) Vertical settlement device C in crushed sand rock zone-8
(*b*) Vertical settlement device A in the compacted river Bed material zone-5

The cumulative consolidation of a lift (9 m thick) upto a particular date was converted to compression in percent of the total initial height of the vertical interval. Values of percent compression for successive dates were plotted against corresponding effective vertical stresses at the mid-height of the lift to form the field compression curves (Figures 15 to 17).

Unmeasured vertical compression occur because first measurements are taken when the fill has been raised by about 3.15 above the mid-height of a lift between two cross arms, when cross arm interval is 1.5 m, or about 6.30 m, when cross arm interval is 3.0 m. The vertical interval between two adjacent cross arms was kept 3 m, it was therefore considered that the first measured increment of compression corresponds to an increase in stress at the mid-height of a lift from approximately 1.4 kg/cm^2. On this basis, it was decided that an allowance for unmeasured compression to the extent of 0.5 percent be made in the measured compression at different instants of time. Therefore field percent compression curves plotted in Figures 15 to 17, are to be added by 0.5 percent to arrive at the value of total percent compression of a lift at a particular value of effective stress. The amount contributed by shear deformation to the decrease of the vertical distance between cross arms was considered small compared to the contribution of one dimensional consolidation.

USBR–Type measuring torpedo was employed for measurements of settlements in telescoping pipe system. A simple and cheap measuring torpedo shown in Figure, 14 (*a*) was devised at the project and was also used for the same purpose. Measurements were made by lowering the torpedo fastened to a surveyor tape to a few centimeter below the approximate elevation of the measurement point (bottom edge of 38 dia cross arm pipe). The device was then pulled taut (by means of nylon thread attached to it) until the pointed end caught under the cross arm pipe and the distance read to a known surface elevation. The tool comes in vertical position and releases from the measuring point, when the pull on the nylon thread is released because of the off-centre balance. The torpedo is further lowered in telescoping pipe system to make measurments at other measurment points.

Interpretation of Field Compression Curves obtained from Vertical Devices

Field compression curves obtained from the observations recorded from Devices *A*, *B*, *C*, *D*, *E* and *F* have been shown in figures 15 to 17, respectively.

Intensities of pore pressures observed from piezometer nos. 10, 18, 29, 36 and 43 have been plotted with respect to measured field compression of 9 m vertical lift between cross arms I and IV and VII to X of Devicc '*B*', cross arms I and IV, cross arms VII to X and XIII to XVII of Device 'E', respectively and shown as curve no. 4, 5, 6, 7 and 8 in Figure 18, respectively. The measured compression at any instant of observed pore pressure was added by 0.5 percent for giving allowance for unmeasured compression. The lowest cross arm of Device '*B*' is located at *El* 255.175 m while piezometer no. 8 at *El* 351.5 m, it was assumed that the field compression at *El* 251.50 m would be 0.5 percent more than measured compression of vertical lift between cross arms I to IV and on this basis observed pore pressure versus measured compression curve at location of piezometer no. 8 was also drawn (Curve no. 3).

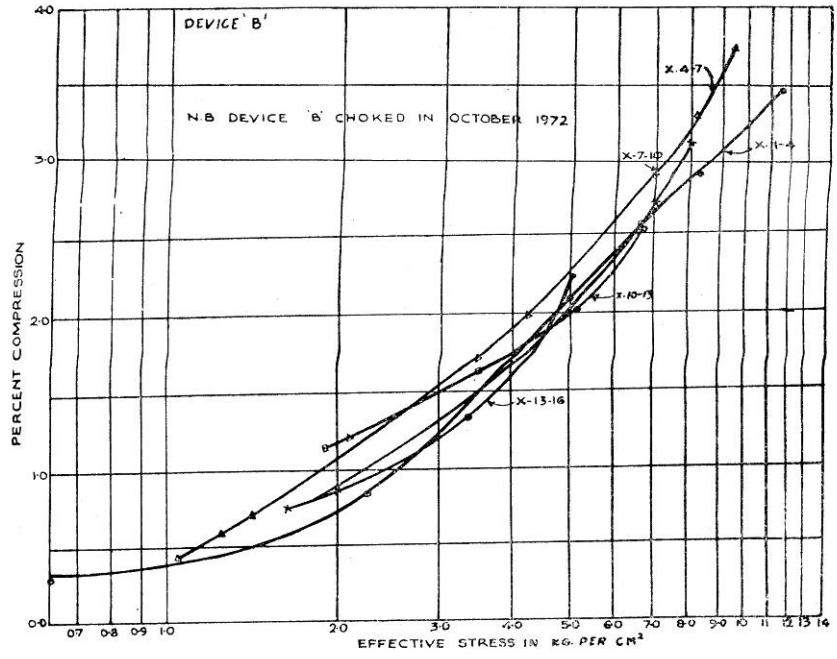

FIGURE 16. Field Compression Curves obtained from
(*a*) Vertical settlement device B
(*b*) Vertical settlement device D in clay core

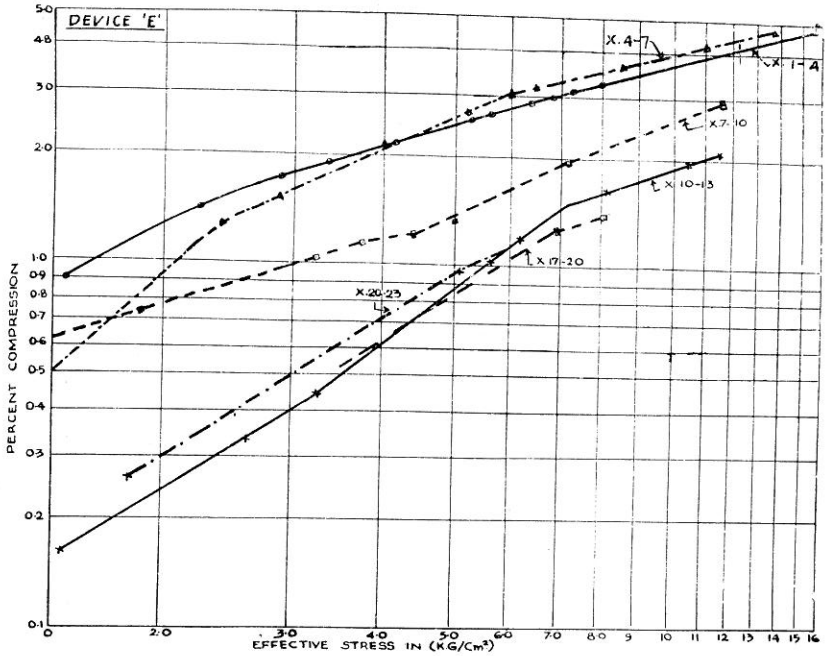

(a)

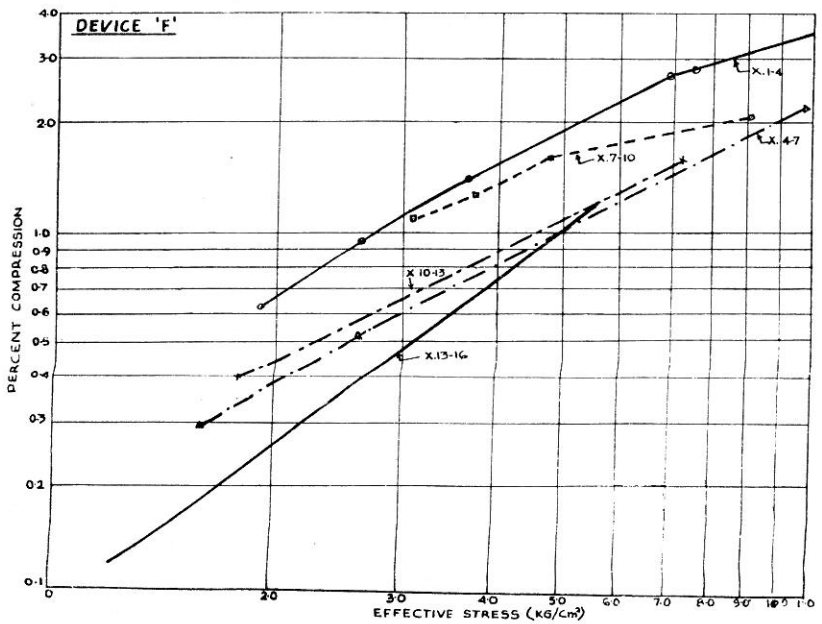

(b)

FIGURE 17. Field Compression Curves obtained from
(*a*) Vertical settlement device E
(*b*) Vertical settlement device F in clay core

The statistical data reveals that the clay fill was placed at average dry density of 2 gm/cm³ and moisture content of 10.5 percent. On the basis of Hilf's Formula, theoretical pore pressure versus percent compression curves were drawn at moisture content of (*i*) 10.5 percent and (*ii*) 12 percent and shown as curve no. 1 and 2 (Figure 18).

Following characteristics were noticed:

(*a*) The field compression curves of Device '*B*' (Figure 16) are quite close and parallel to each other indicating that various lifts were placed at uniform moisture content and compaction. These are concave curves with low initial strain and constant or slightly increasing compressibility at loads higher than 2 kg/cm².

(*b*) The field compression curves of Device '*D*', '*E*' and '*F*' (Figures 16 and 17) are convex upwards, but are fairly straight in initial reaches. This shows that clay which was placed near optimum had uniform compressibility at moderate effective stresses (1 to 10 kg/cm²) followed by decreasing compressibility at higher effective stresses.

(*c*) The compressibility of the lowest 9 m vertical lift resting on rock has generally been found to be maximum (Figures 15 to 17). The compressibility of second lowest lift at the same intensity of effective stress is generally found to be lesser than first lowest, while third lesser than second and so on (with one or two exceptions). This shows that the compressibility of vertical lifts at lower depths at any particular intensity of effective stress shall be greater than those at higher locations, while the maximum shall be of the one directly resting on rock, even though compaction and moisture content of all the layers may be the same. This phenomenon can be attributed to various modes of load transfer and changes in modes at different elevations and different locations of the embankment.

(*d*) The increase in the compressibility of lower vertical lifts of Device '*A*' and '*C*' (Figure 15) located in upstream and downstream outer shells, with increase in overburden stress can be in part due to higher shear strains at lower depths along outer slopes.

(*e*) Field compression curves of Device *C* (Figure 15) located in crushed sand rock zone–8 (placed 4 to 6 percent drier than optimum) are concave upwards with low initial strain and slightly increasing compressibility so that in all instances, compressibility is maximum at the end of construction. A fill compacted sufficiently drier than optimum have been found to exhibit such characteristics (Gould 1954).

(*f*) Observed pore pressure versus measured percent compression curves (of piezometer nos 8 and 10) in their initial reaches are fairly close to theoretical curve drawn at 12 percent moisture content of the fill; this confirms that the moisture content of the fill at these locations was about 12 percent and that the clay core was wetted by river water during monsoon period of year 1969. All the free soil in a soil mass containing 12 percent moisture content at density of 2 gm/cm³ shall be driven into solution at 1.9 percent

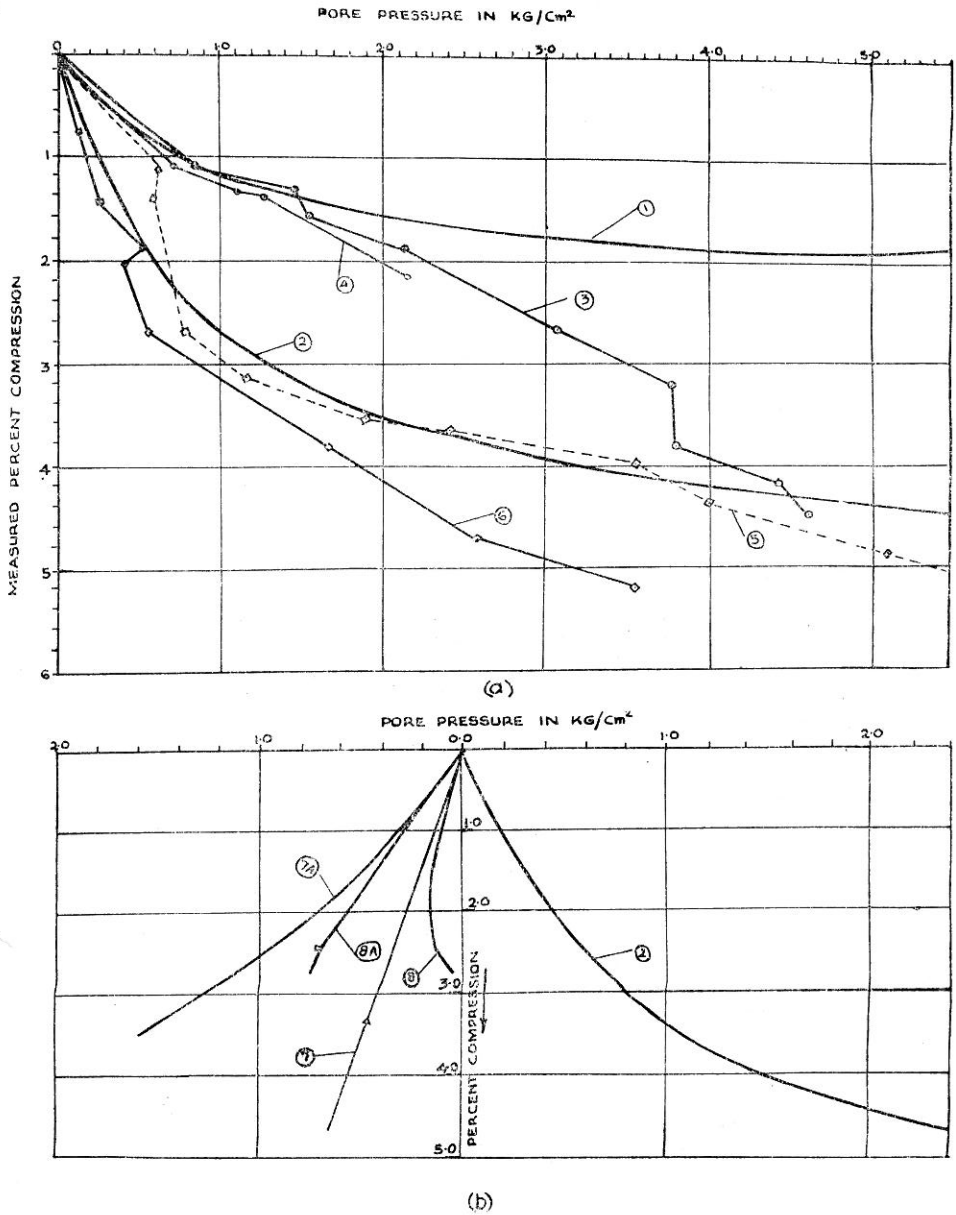

FIGURE 18. Pore pressure vs Measured percent compression curves for
(*a*) Piezometer nos. 8, 10, 18 and 29
(*b*) Piezometer nos. 36 and 43.

compression which took place in April '71 (Figure 5). The clay fill at this location thus, became saturated in April '71. Any further increase in superimposed load should be reflected by an equal rise in pore pressure. However it is not noticeable in pore pressure curve of piezometer no. 8 indicating drainage of water from clay core towards encasing sand rock zones. The activity of drainage after saturation resulted in significant increase in percent compression of fill layers (Figure 5).

(*g*) Observed pore pressure curves (Figure 18) for piezometer no. 18 and 29 are quite close with theoretical pore pressure curves drawn for 10.5 percent moisture content of the fill confirming that the fill was laid at moisture of 10.5 percent at these locations.

(*h*) It can be seen that the activity of drainage of water in clay fill near piezometer no. 8 is greater than activity of drainage of air in clay fill near piezometer no. 18 and 29 (Figure 18). This indicates that water, due to its additional capacity of wetting the soil particles has a higher capacity of penetrating into the soil than the air.

(*i*) All the free air in the soil adjoining piezometer no. 18 shall be driven into solution when the measured settlement equals the percentage of air (4.8 percent). This took place by the completion of main dam and therefore clay fill below *El* 300 m became saturated. In such circumstances the clay fill below *El* 300 m shall not obviously experience additional settlement upon penetration of reservoir seepage, except that due to reservoir load on upstream face. This shows that the heavy compactive effort to attain Proctor's maximum density and placement moisture content near optimum in case of high dams influences in preventing the tendency of compression of clay core when penetration of reservoir seepage takes place.

At higher values of pore-pressures, the activity of drainage appears to be intensified (Figure 18).

(*j*) The capillary stresses (curve nos. 7A and 8A) at a particular instant of compression has been calculated, by adding the theoretical pore air pressures to observed value of negative pore pressure (Curve no. 7 and 8 in Figure 18). The result shows that capillary stresses to the extent of 1.43 kg/cm^2 developed in clay core at higher elevations.

(*k*) It can be seen from figure 19 that the core experiences greater settlements than the outer shells on a particular date; this shall result in development of differential movements between core and the outer shells.

Upstream-Downstream Horizontal Strain within the Embankment

Internal Horizontal Movement Devices were installed as a part of the telescoping vertical movement cross arm devices *A*, *B*, *C*, *D* & *E*. Horizontal movement of plates is transformed into vertical movement by a linkage system and is obtained by measuring torpedo and reading scale when

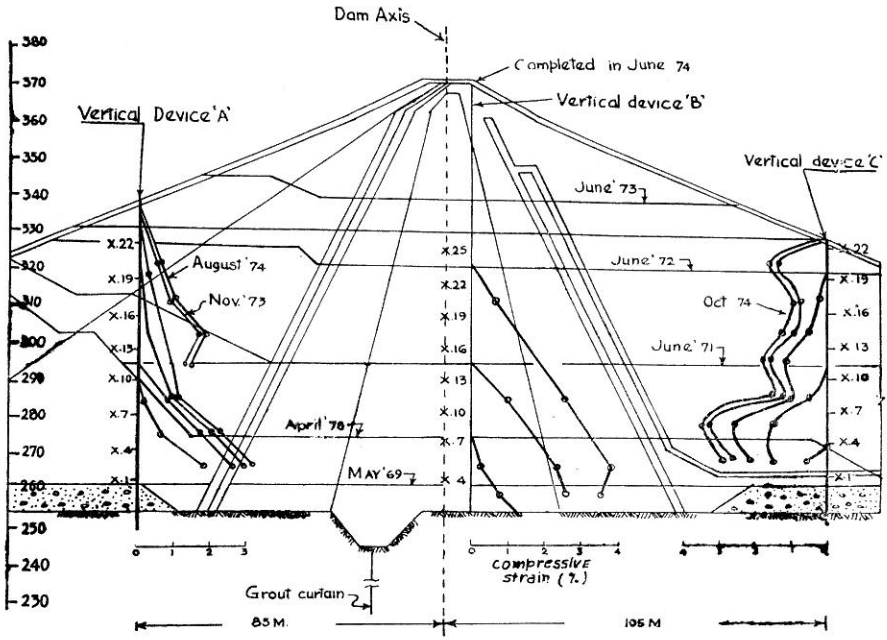

(a)

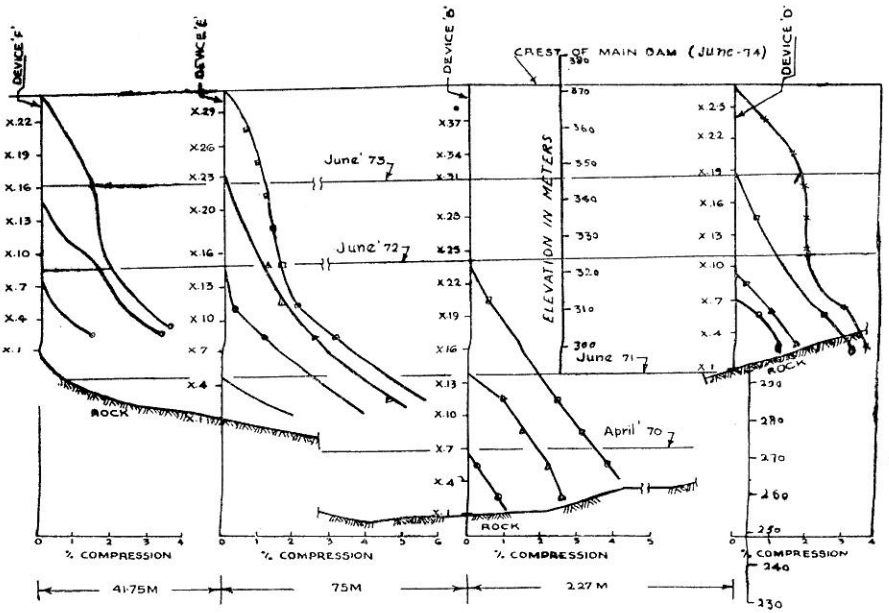

(b)

FIGURE 19. Distribution of compressive strain within dam embankment of different dates

pawls of torpedo engage the lower ends of 37 mm dia pipe (1), Counterwell no. 1 (2) and counterwell no. 2 (3), as shown in Figure 20*a*. The original distance between '1' and '2' (L_1) and also '1' and '3' (L_2) is calculated from initial readings, while the changed distance between '1' and '2' (L'_1) and '1' and '3' (L'_2) at any instant from subsequent readings. The change in distance between the horizontal movement plates is then given by :

$$\triangle L=(L_1-L'_1)+(L_2-L'_2)$$

Then percentage horizontal strain is given by:

$$\frac{\triangle L}{L}\times 100=\frac{(L_1-L'_1)+(L_2-L'_2)}{L}\times 100$$

Where, L = Distance between the horizontal movement plates (generally 6 m).

It can be seen from figure 20(*a*) that horizontal strain is generally compressive in nature. Only horizontal movement devices installed at *El.* 325.34 m and 348.88 in vertical Device '*E*' and *El* 366.705 m in vertical Device '*D*' have recorded tensile horizontal strain, within the clay core. Tensile horizontal strain has also been recorded by horizontal movement device installed at *El* 291.530 m in Device '*A*' in Zone 5 (upstream outer shell) from Oct. '71 to Oct '72 and by horizontal device installed at *El* 292.75 in Device '*C*' in Zone 8 (downstream outer shell) from April '71 to January '70.

Percent horizontal strain is maximum in horizontal movement devices installed in vertical Devices '*A*' and '*C*' (at *El* 315.48 m and 292.715 m, respectively), as these are located in outer zones of the dams, where contribution of shear strain is maximum, while it is quite low in Devices *B*, *D*, *E*, and *F* located in clay core. Nominal changes in horizontal strain are also taking place after completion of the dam due to reservoir filling and depletion.

The maximum percent horizontal strain in the clay core is only 0.25% which shows that the decrease in volume of soil mass practically took place in vertical dimension only. Horizontal strain is compressive in nature in clay core at lower elevations, while tensile in nature at higher elevations. The clay fill at lower elevations experienced compressive upstream-downstream horizontal strain due to stronger encasing material in outer zones.

Stress Distribution within Main Dam

Twelve stress meters were installed within Main Dam embankment at different locations. A group of four stress meters was installed at one location (6.9 m upstream of dam axis and at *El* 304 m) in clay core along deepest river bed section. One of these four stress meters was laid flat (1) determining the intensity of normal stress within clay core. The other three, one parallel to dam axis (2), one perpendicular to dam axis (3) and the third inclined 45° to dam axis (4) were laid vertically such that the stress sensing sides are exerted by horizontal stress developing within clay core (Figure 21) and record horizontal stress. A similar group of four stress meters was similarly installed in zone 2-*b* (sand rock-core) near right

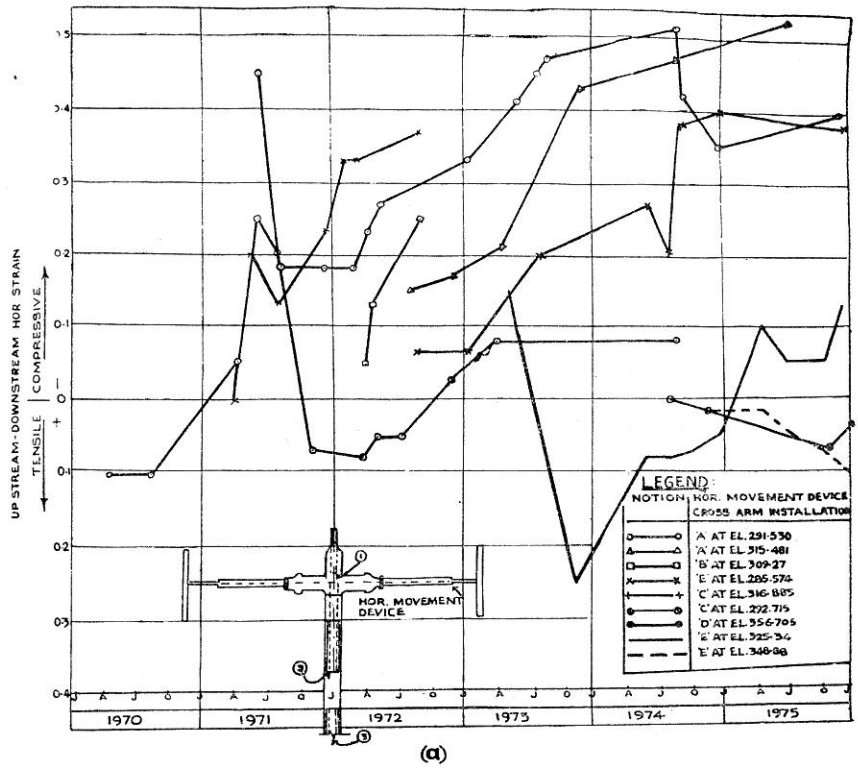

(a)

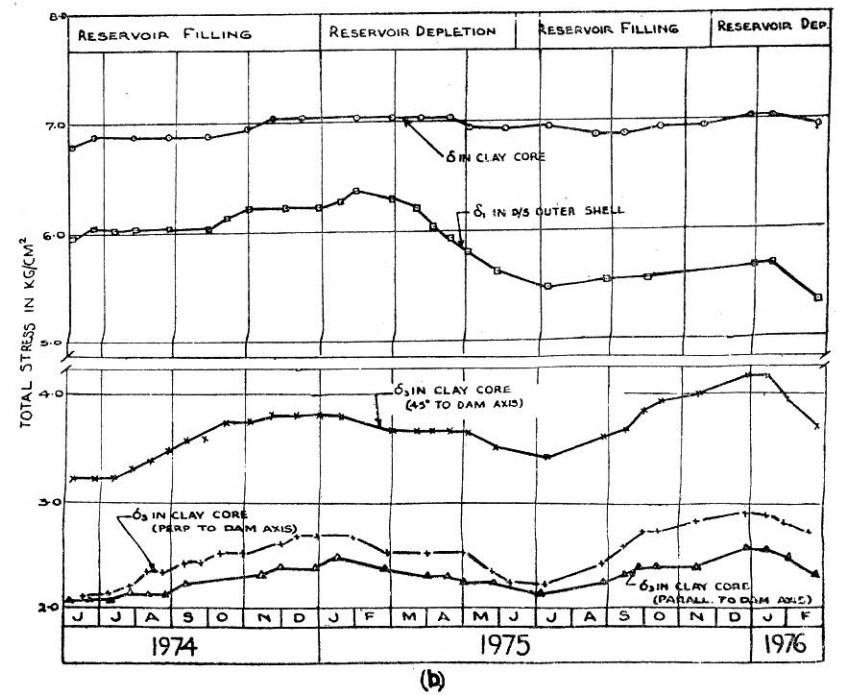

(b)

FIGURE 20. (*a*) Upstream—downstream horizontal strain within dam embankment
(*b*) Stress variation within main dam during reservoir filling

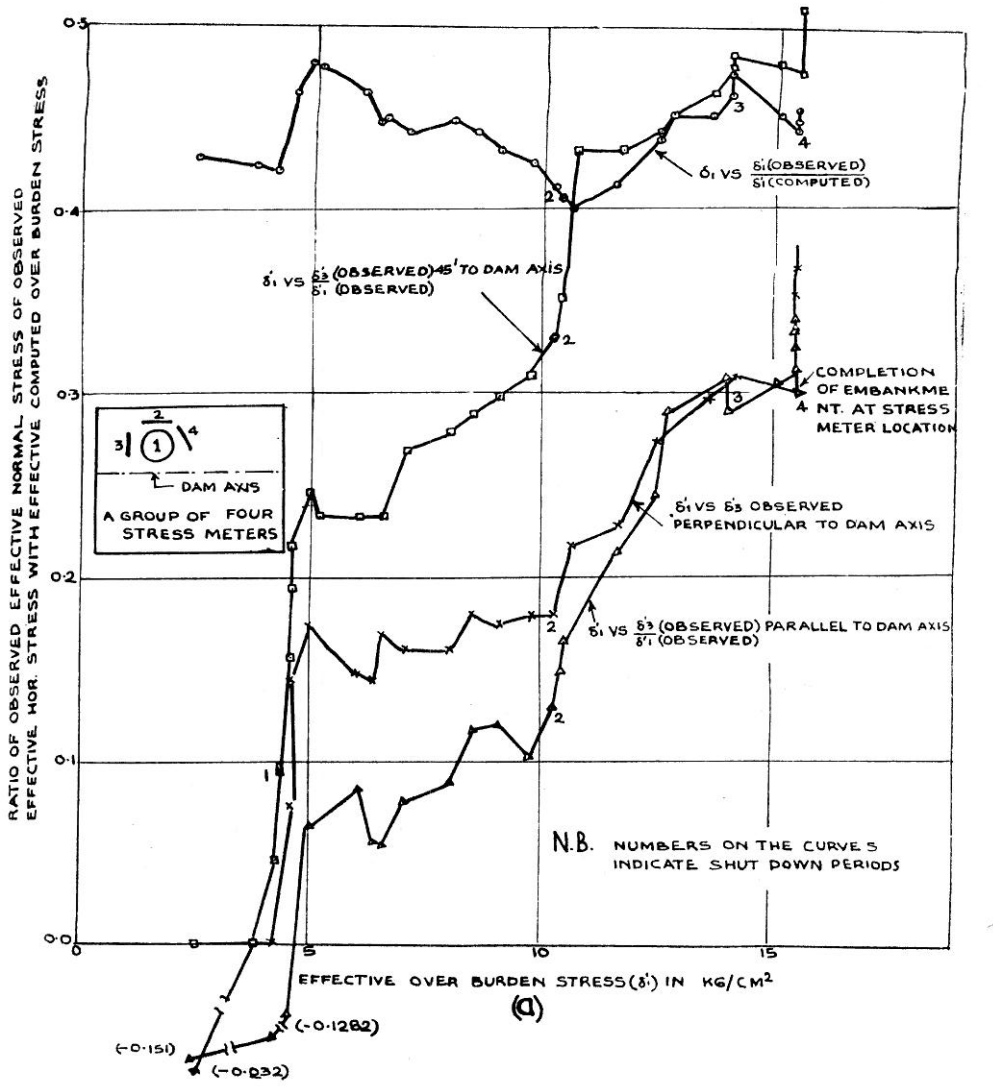

FIGURE 21. Variation of normal and horizontal stresses in clay core during construction recorded by stress meters

abutment. One stress meter in Zone-8 crushed sand rock (at 94 m downstream of dam axis and at *El* 298.8 m) and two in clay core at *El* 350 near the vertical face of chute spillway wall and one in clay core at *El* 300 m near left abutment were laid flat for determining the intensity of normal stress within the dam.

Following stress distribution within Main Dam was noticed:

(*a*) Ratio of measured effective normal stress to computed effective normal stress (on the basis of height of overburden and the observed pore pressure) is on average only 0.45 (Figure 21) due to following reasons:

(*i*) Clay core is flexible and compressible and is encased by stronger materials in outer zones. The encasing material produces compressive stresses in clay core resulting in phenomenon of load transfer from weaker materials (clay core) to stronger materials (outer zones).

(*ii*) Cross valley displacements take place due to occurrence of greater vertical settlements in the same layer in deepest portion than that near abutments which result in phenomenon of load transfer from deepest portion to towards abutments.

(*iii*) Certain proportion of superimposed loads of embankment placed in central zone disperses towards outer zones.

(*iv*) Bridging effects occur in clay core due to change of modulii of elasticity of clay layers at different depths and effect changes in mode of load transfer.

(*v*) When the measuring points consist of materials of different modulii of elasticity, which depending on the position may differ more or less from the modulii of earth pressure cells, 'bridging effects' result in a specific pressure too low at the measuring membrane.

Factory calibration is made by observing the change in frequency of the transmitter (placed in a water filled container) at different known intensities of water pressures. It has been reported that calibration of the same transmitter, when encased in saturated sand surrounded by water, may give different results. Therefore every stress meter should be calibrated after covering it in the respective fill material placed in a box at defined application of load. This calibration would be done at Kalagarh Laboratory on receipt another stress meter from M/s Maihak, West Germany for determining correction factor for respective fill materials.

(*b*) Horizontal stresses did not develop in the embankment for intensities of computed effective stresses up to 4 kg/cm^2.

(*c*) The ratio $\frac{\sigma_3(\text{observed})}{\sigma_1(\text{observed})}$ showed increase with increase in the intensity of effective stresses (where σ_1 is effective normal stress, while σ_3 effective horizontal stress).

(*d*) In general, the ratio of observed stress with computed overburden stress at stress meter location decreases while fill is raised after shutdown periods, but the ratio again increases after some time. This shows that the delayed lateral transfer of load of the added fill height after shutdown took place and this resulted in the value of the increments in measured stress to be lower than the corresponding increase in the fill weight. It may also be seen that increase in measured stress was recorded during third shutdown period when the fill height remained the same. This shows that the lateral transfer of fill load added in the period before shutdown, was taking place slowly during shutdown periods. The delayed lateral transfer of the load was responsible for increase in intensities of pore pressures and settlements during shut down periods.

(*e*) The ratio $\frac{\sigma_3(\text{observed})}{\sigma_1(\text{observed})}$ is maximum in direction 45° to dam axis least in direction parallel to dam axis.

The intensities of normal stresses and horizontal stresses increase during reservoir filling, but these decrease during depletion of reservoir (Figure 20 *b*). This clearly demonstrates that stresses in clay core are affected by reservoir load on the upstream face of the dam.

The effect of reservoir load is also noticeable in the observed intensities of normal stress in downstream outer shell (Figure 20 *b*). This shows that downstream horizontal displacement of dam taking place due to reservoir load increases the normal stress in downstream outer shell.

(*f*) The ratio (R_1) between observed effective normal stress and computed effective normal stress in zone-8 (downstream outer shell) is on average 0.75 when computed stress is between 3.6 to 6.3 kg/cm² (Figure 10). R_1 was 0.785, when desired fill elevation (335.2 m) reached in April 73 at the location vertically above the stress meter location. The dispersal of added load of embankment above *El* 335.2 m was responsible for increase in observed effective normal stress at stress meter location and therefore the value of R_1 became 0.98 at the end of completion of Main Dam. The value of observed normal stress in zones-8 at (*i*) fill elevation 335.2 m was 4.72 kg/cm² (*ii*) fill elevation 348 m was 5.38 kg/cm² (*iii*) fill elevation 372m was 5.96 kg/cm². According to charts of Osterberg, (Osterberg, 1957) the increase in observed normal stress at stress meter location due to rise in embankment elevation from 335 2 m to 348 m comes to 0.66 kg/cm² (against observed increase of 0.69 kg/cm²) while due to rise in embankment elevation from 335.2 m to 372 m, comes to 0.92 kg/cm² (against observed increase of 1.24 kg/cm²). The two results are fairly comparable and show that the dispersal of loads to outer zones took place.

(*g*) The stress meter located in clay core near the vertical face of chute spillway has recorded normal stress equivalent to computed stress (Figure 10).

The above study reveals that various modes of load transfer and changes in modes may occur in an embankment during its life time.

It shall obviously influence the characteristics of embankment behaviour—settlements and cross valley displacements, strains, pore water pressures and earth pressures.

Horizontal Displacements within Dam

Total horizontal displacement (in inches) of any point with respect to bottom is expressed by :

$$M = 0.0035 \Sigma \triangle \text{Dial}$$

Where (*i*) $\triangle$ Dial = [$(D_n - D_s)$ new reading $-(D_n - D_s)$ initial reading], (*ii*) D_n = slope Indicator Dial reading in north groove, (*ii*) D_s = slope Indicator Dial reading in south groove.

Vertical dark lines (in Figure 22) show the apparent initial position of the casing pipes at the time of installation. The horizontal distance between vertical lines and curves representing the position of casing pipes on subsequent dates, represent the horizontal displacement of the fill.

To divert the monsoon inflows through diversion tunnels, first stage dam (Figure 2) was constructed by June 1970; its section included the placement of materials in zone-5 to El 344 while of the materials in core and downstream outer shell to El 275 m only. Subsequently the core was raised along with downstream zones and remaining portion of upstream zones in following years. Thus only a part of upstream outer shell raised along with core, applied confining pressures on the core on its upstream side, while the whole of the downstream outer shell applied confining pressures on downstream side of the core. This resulted in greater confining pressure on the core from downstream side than from the upstream side. The unbalanced confining forces shall obviously result in upstream (north) horizontal displacement of the core and therefore the clay core experienced horizontal displacement in upstream (north) direction during construction (Figure 22); its maximum value at the end of completion of main dam being 38.5 cm and 31.5 cm at the deepest river bed section and near right abutment, respectively.

The reservoir was impounded to El 340 m by January, 1974 and therefore the core experienced horizontal displacement of about 18 cm in downstream (south) direction. The core again experienced horizontal displacement of about 5 cm in downstream direction, when the reservoir was *filled for the second time to El 355 m by December 1975.*

The horizontal displacements in clay core near right abutment in east—west direction (generally termed as cross valley displacements), took place in East direction (Figure 23) i.e. towards centre of the valley while in clay core near left abutment in west direction i.e. again towards centre of the valley. The cross valley displacements at lower elevations of the right abutment are greater in intensities than those near left abutment. The right abutment steeply rises from the deepest valley portion, while the left abutment is intercepted by a level terrace before its steep rise (Figure 2). This topographical feature was probably responsible for producing greater cross valley displacements in clay core near right abutment. Cross displacements take place due to greater normal settlements of the same layer of embankment in deepest river bed section than that in other portions and this influences change in mode of load transfer.

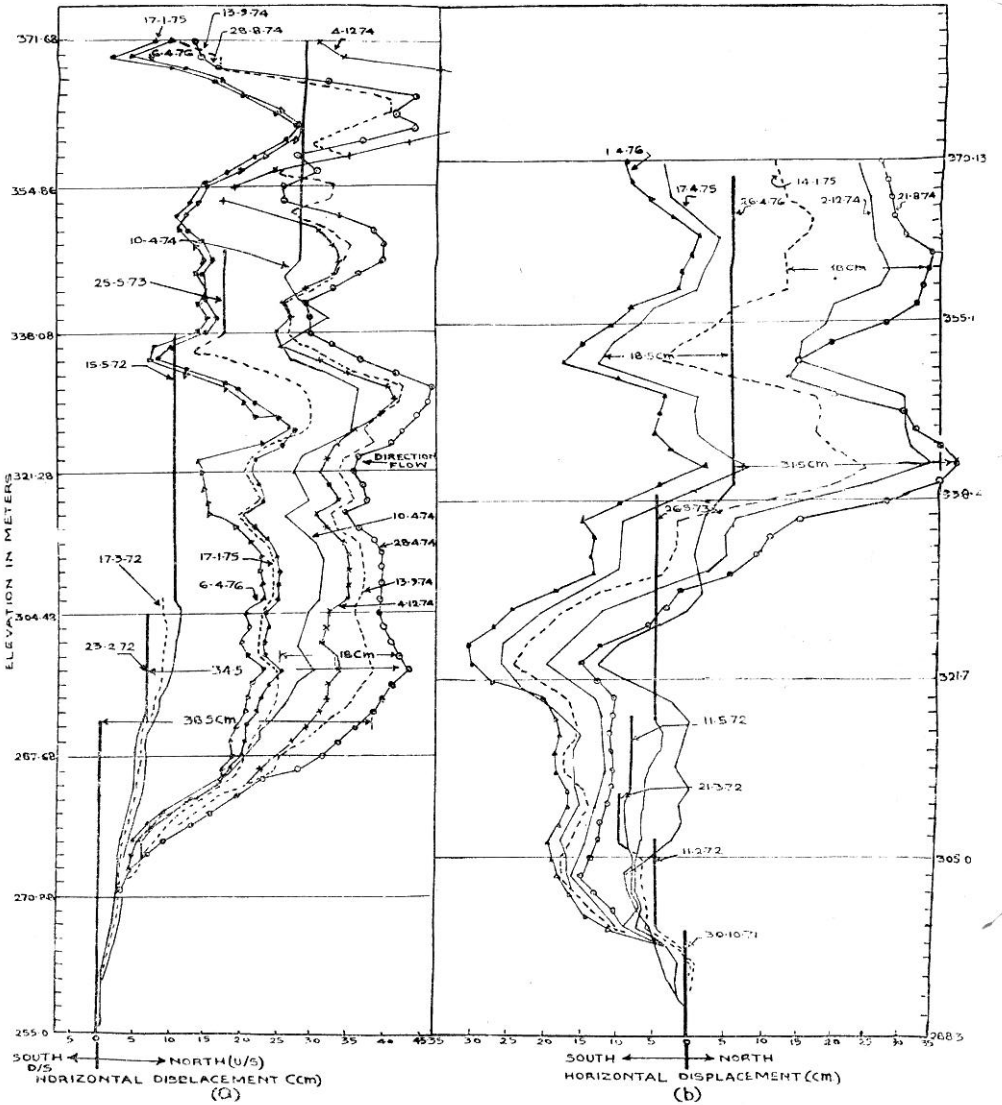

FIGURE 22. Horizontal displacement in north-south direction recorded by slope indicators installed (*a*) at deepest riverbed section in clay core, 9.5 m downstream of dam axis (*b*) near right abutment in clay core, 12 m downstream of axis

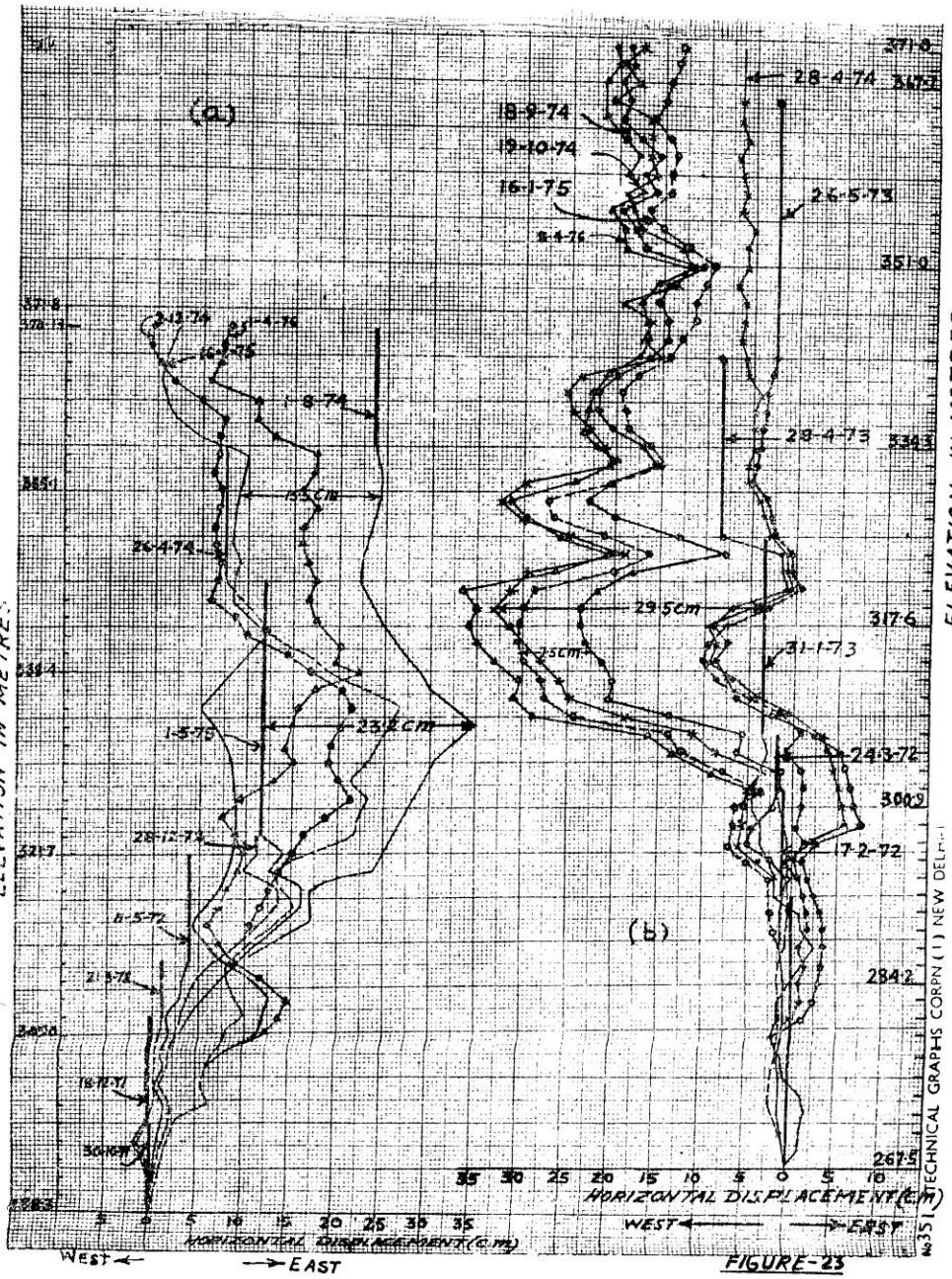

FIGURE 23. Horizontal displaccment in east-west direction recorded by slope installed near (*a*) right abutment in clay core, 12 m downstream of dam axis (*b*) left abutment in clay core 15 m upstream of dam axis

The core also experienced changes in the intensities of cross valley displacements during the reservoir filling; the changes in the intensities between the period from August 1974 to January 1975, were about 15.5 cm and 7.5 cm in the core near right abutment and left abutment, respectively. The changes in intensities of cross valley displacements during reservoir filling therefore would again result in change of mode of load transfer within the embankment and influence the embankment behaviour-*settlements, pore pressures and stress distribution.*

Conclusions

The observed pore-pressure data from Ramganga Main Dam was analysed to indicate the development and magnitudes of construction pore-water pressures and seepage pore water pressures in Ramganga Dam. Factors which affect the build up of construction pore pressures are numerous. Placement water content, overburden weight, nature of fill material, permeability and volume of air in pores of compacted fill material, length of drainage path, rate of construction including construction shut down periods, presence of drainage features, field compression characteristics of the fill materials, cross-valley displacements, change in mode of load transfer, all exert some effect. Because of the interdependence of all these factors, it is difficult to isolate the relative influence of any one factor on the development of construction pore pressures.

The coefficient of compressibility of the rock fill or boulderfill and shape of field compression curves depend on (*i*) type of material (*ii*) moisture content (*iii*) balance of weight below 0.08 mm particle sizes (*iv*) the shape of the valley which influences development of cross valley displacements and thereby alters the field compression characteristics (*v*) height of overburden (*vi*) differential movements between core and shell.

The compressibility of crushed rock fill layers at lower elevations near abutments will be higher than those at higher elevations of the embankment even though effective stress, moisture content, density and the type of the material may remain the same. The contribution of shear deformation is small, compared to that of one dimensional consolidation. Upstream-downstrem horizontal strain is maximum at outer slopes of the dam where influence of shear deformation is significant due to no lateral restraint. The clay fill experiences compressive upstream-downstream horizontal strain due to stronger encasing material in the outer zones.

Cross valley displacements take place in the fill, these shall be higher where abutment is steep. The stronger encasing material assists in development of compressive stresses in the core. The dispersal of load of embankment takes place increasing normal stresses in areas of outer zones even though not lying vertically below the loaded area. The bridging effect due to change of modulii of elasticity at different depths of fill is also responsible in recording pressures on the lower side. All these factors affect change in mode of load transfer which significantly influence the embankment behaviour-settlements, cross valley displacements, strain, pore-water pressures and stress distribution.

The reservoir load induces horizontal displacement (in downstream direction) in the core fill. It also influences changes in cross valley displacements; indicating change in mode of load transfer even during reservoir filling.

Consolidation under reservoir load and due to dissipation of pore pressures in the core of Main Dam which was laid near optimum (10.5 per cent), took place. No significant tendency to compression on saturation has been observed in Main Dam core, indicating the influence of the heavy compactive effort and placement moisture content near optimum in preventing it.

References

BISHOP, A.W., (1957), "Some Factors Controlling Pore Pressure set up during Construction of Earth Dam", *Fourth International Conference on Soil Mechanics and Foundation Division*, London, Proceedings, Volume II, Page 294-300.

EARTH MANUAL., (1974), *United States Department of Interior, Bureau of Reclamation*, Second Edition.

GOULD, J.P., (1954), "Compression Characteristics of Rolled Fill Materials in Earth Dams", *Technical Memorandum No. 648*, Bureau of Reclamation, United States Department of the Interior, Denver.

GOULD, J.P., (1959), "Construction Pore-Pressures observed in Rolled Earth Dams", *Technical Memorandum No. 650*, Bureau of Reclamation United States Department of Interior, Denver.

HILF, J.W., (1956), "An Investigation of pore-Water Pressures in Compacted Cohesive Soils", *Technical Memorandum No. 654*, Bureau of Reclamation, U.S. Department of Interior, Denver.

HILF, J.W., (1948), "Estimating Construction Pore-Pressures in Rolled Earth Dam", *Second International Conference on Soil Mechanics and Foundation Engineering*, Proceedings, Volume-III page-234.

HIRSCHFELD, R.C. and POULOS, S.J., (1973), "Embankment-Dam Engineering", Casagrande Volume, A *Whiley-Interscience Publication*, John Willey and sons, New York.

KULHAWY, F.H., and DUNCAN, J.M., (1972), "Stresses and Movements in Oroville Dam", *Journal of Soil Mechanics and Foundation Division, ASCE*, Vol. 98, No. SM 7, proceeding paper 7513, pp 653-665.

LAMBE, T.W., (1961), "Residual pore pressures in Compacted clay", *XXV International Conference on Soil Mechanics and Foundation Engineering*, Paris, Proceedings, Volume I, pp-207.

LI, C.F., (1959), "Construction Pore Pressure in an Earth Dam" ASCE, *Journal of Soil Mechanics and Foundation Division*, Vol. 85, No. S.M. 5, Proceeding Paper 2213, pp. 43-59.

LI, C.F., (1967), "Construction Pore Pressures in Three Earth Dams", ASCE, *Journal of Soil Mechanics and Foundation Division*, Vol. 93, No. S.M. 6, Proceeding Paper 5122, March.

MARSAL, R.J. and ARELLANO, L.R.D., (1973), "Field Measurements in Rockfill Dams", *Proceedings, 2nd Pan American Conference on Soil Mechanics and Foundation Engineering*, Vol. II Sao Panlo.

MARSAL, R.J. and ARELLANO, L.R.D., (1967), "Performance of El Infiernillo Dam", 1963-66, *Journal of Soil Mechanics and Foundation Division, ASCE*, Vol. 93, No. S.M. 4, Proceeding Paper 5318, pp. 265-298.

NEWLIN, CHARLES W. and ROSSIER, STANLEY C., (1976), "Embankment Drainage After Instantaneous Drawdown", *Journal of the Soil Mechanics and Foundation Division, ASCE*, Vol. 93, No. S.M. 6, Proc. Paper 5567, November, pp. 79-85.

OSTERBERG, J.O., (1957), "Influence Values for Vertical Stresses in a Semi-infinite Mass Due to an Embankment Loading", *IV International Conference on Soil Mechanics and Foundation Division*, London, Proceedings, Volume I, pp. 393.

RADLEY SQUIER., (1970), "Load Transfer in Earth and Rock Fill Dam", Proceedings of ASCE, *Journal of Soil Mechanics and Foundation Division*, Vol. 96, No. S.M. 1, January, pp. 213-233.

ROURKE, J.E., (1974), "Performance Instrumentation Installed in Oroville Dam", *Journal of Geotechnical Engineering Division, ASCE*, Vol. 100, No. GT 2, February.

SHERARD, J.L., et al., (1967), others, "Earth and Earth-Rock Dams" *John Willey and sons.*

SOYDOMIR, C., and KJNERNSLI, B., (1975), "A Treatise on the Performance of Rockfill Dams with Unyielding Foundations in Relation to the Design of Storvass Dams", 53203, *Norges Geotechniske Institute*, November.

SHERMAN, W.C., and CLOUGH, G.W., (1968), "Embankment Pore Pressures During Construction", *Journal of Soil Mechanics and Foundation Division (March)*, Proceedings, ASCE, Vol. 94, No. S.M. 2 Proceeding Paper 5867, pp. 527-553.

Technical Memoranda, "Analysis and Interpretation of Instrumentation Data of Ramganga Dam" End of Construction Period—September 1974 and Reservoir Filling Period June 1975, *Central Water Cemmission*, New Delhi.

WILSON, S.D., (1967), "Investigation of Embankment Performance" *Journal of Soil Mechanics and Foundation Division*, ASCE, Vol. 93, No. S.M. 4, Proceeding Paper 5311, July pp. 135-156.